ORIGINAL ARTICLE

Soil Science Society of America Journal

Fundamental Soil Science

Estimates of soil taxonomic change due to near-surface permafrost loss in Alaska

N. A. Jelinski¹ N. J. Pastick² A. L. Kholodov³ M. J. Sousa⁴ J. M. Galbraith⁵

²U.S. Geological Survey, Earth Resources Observation and Science Center, Sioux Falls, South Dakota, USA

³Permafrost Laboratory Geophysical Institute, University of Alaska-Fairbanks, Fairbanks, Alaska, USA

⁴USDA Natural Resources Conservation Service, Wasilla, Alaska, USA

⁵School of Plant and Environmental Science, Virginia Polytechnic Institute and State University, Blacksburg, Virginia, USA

Correspondence

Nicolas Jelinski, Department of Soil, Water and Climate, University of Minnesota Twin-Cities, 1991 Upper Buford Circle, Saint Paul, MN 55108, USA. Email: jeli0026@umn.edu

Assigned to Associate Editor Dylan Beaudette.

Funding information

USDA Natural Resources Conservation Service Award, Grant/Award Number: NR223A750025C013; National Science Foundation Award, Grant/Award Number: ICER-2129363

Abstract

Gelisols (permafrost-affected soils in US Soil Taxonomy) are extensive in Alaska, currently occurring on \sim 45% of the land area of the state. Gelisol taxonomic criteria rely on the presence of near-surface (less than 2 m deep) permafrost, but ongoing climatic and environmental change has the potential to affect the presence of near-surface permafrost across much of Alaska throughout the 21st century. In this study, we utilized scenarios of near-surface permafrost loss and active layer deepening through the 21st century under low (SRES B1, RCP 4.5), mid- (SRES A1B), and high (SRES A2, RCP 8.5) emissions scenarios, in conjunction with the statewide STATSGO soil map, to generate spatially explicit predictions of the susceptibility of Gelisols and Gelisol suborders to taxonomic change in Alaska. We find that 15%-53% of Alaskan Gelisols are susceptible to taxonomic change by mid-century and that 41%-69% of Alaskan Gelisols are susceptible to taxonomic change by the end of the century. The extent of potential change varies between suborders and geographic regions, with Gelisols in Northern Alaska being the most resilient to taxonomic change and Western and Interior Alaskan Gelisols most susceptible to taxonomic change. The Orthel suborder is likely to be highly restricted by the late 21st century, while Histels and Tubels are more likely to be of greater extent. These results should be taken into consideration when designing initial survey and re-mapping efforts in Alaska and suggest that Alaskan Gelisol taxa should be considered threatened soil taxa due to the proportional extent of likely loss.

Abbreviations: CMIP, Coupled Model Intercomparison Project; CV, coefficient of variation; DOS-TEM, Dynamic Organic Soil version of the Terrestrial Ecosystem Model; GCM, global climate model; GIPL, Geophysical Institute Permafrost Laboratory; gNATSGO, Gridded National Soil Survey Geographic Database; LRR, land resource region; NSP, near-surface permafrost; QTP, Qinghai-Tibet Plateau; RCP, Representative Concentration Pathway; SNAP, Scenarios Network for Alaska Planning; SRES, Special Report on Emissions Scenario; SSP, Shared Socioeconomic Pathway; SSURGO, soil survey geographic database; STATSGO2, State Soil Geographic Dataset.

This is an open access article under the terms of the Creative Commons Attribution-NonCommercial License, which permits use, distribution and reproduction in any medium, provided the original work is properly cited and is not used for commercial purposes.

© 2024 The Author(s). Soil Science Society of America Journal published by Wiley Periodicals LLC on behalf of Soil Science Society of America.

¹Department of Soil, Water and Climate, University of Minnesota Twin-Cities, Saint Paul, Minnesota, USA

1 | INTRODUCTION

Alaska is experiencing widespread climatic and environmental change, which is predicted to accelerate throughout the 21st century (Grosse et al., 2016) and lead to significant increases in permafrost temperatures, deepening of seasonal thaw depths, and decreases in permafrost extent (Pastick et al., 2015, 2019; Romanovsky et al., 2017). These changes may have profound impacts on infrastructure stability (Hjort et al., 2022), engineering design (Harris et al., 2018), terrestrial carbon storage (Hugelius et al., 2014), agricultural management (Peplau et al., 2022), and ecosystem services (Schuur & Mack, 2018). For these reasons, the identification and classification of soils with permafrost are critically important in soil survey (Bockheim et al., 2006; Rieger, 1983).

The classification of permafrost-affected soils at the highest level (soil order) in US Soil Taxonomy relies on a single diagnostic feature—the presence of permafrost (material which remains at 0°C for at least 2 consecutive years; van Everdingen, 2005)—within 1–2 m of the soil surface (Soil Survey Staff, 2022a). This is a practical boundary due to limitations of observation depth in soil survey (Moore & Ping, 1989) and is reasonable with regard to predicting the most severe and significant impacts on land use, management, and ecological systems (Osterkamp et al., 2009). Permafrost at these depths is best characterized as "near-surface" permafrost (NSP; Pastick et al., 2015) because the depth to and thickness of permafrost in much of Alaska may exceed tens to hundreds of meters (Jorgenson et al., 2008).

The need to group and communicate the properties of soils with NSP for interpretive purposes was the motivating factor behind the creation of permafrost-affected soil taxa (Ahrens et al., 2004; Moore & Ping, 1989; Ping, 2013b; Tarnocai & Bockheim, 2011). These taxa elevate the presence of NSP above all other soil properties and are given primacy at the highest levels of US Soil Taxonomy (Soil Survey Staff, 2022a), the Canadian Soil Classification System (Canadian Soil Classification Working Group, 1998), and the World Reference Base for Soil Resources (WRB, 2022). Grouping permafrost-affected soils into a single class has allowed the generalized prediction of soil and landscape behavior and the comparison, extrapolation, and exchange of soil information across multiple scales (Hugelius et al., 2013; Jones et al., 2009; Tarnocai et al., 2002). Therefore, permafrostaffected soil taxa serve as a bridge connecting NSP extent to interpretations and land-use limitations and have important implications for soil mapping and soil data use efforts in Alaska, where permafrost-affected soils are currently estimated to cover $\sim 40\%$ –50% of the total area of the state (Soil Survey Staff, 2022b).

Users of soil survey depend on the information contained in the major components within soil map units (USDA-NRCS, 2023) and therefore upon the reliability of the soil properties,

Core Ideas

- Fifteen to fifty-three percent of Alaskan Gelisols are susceptible to taxonomic change by 2050– 2059.
- Forty-one to sixty-nine percent of Alaskan Gelisols are susceptible to taxonomic change by 2090– 2099.
- Extent of taxonomic change is the highest in the Interior and lowest in Northern Alaska.
- Susceptibility to change differs by land resource region and Gelisol suborder.

taxonomic classifications, and the interpretations that flow from them (Aandahl, 1958; Soil Survey Staff, 2017). If the properties of a map unit change on the ground, interpretations and classification would undergo important changes that have real-world implications on decision-making. Due to interannual, inter-decadal, and century scale variability in heat transfer and active layer thickness, depth to permafrost is best conceptualized as a dynamic soil property that responds to climatic and environmental forcings (French & Shur, 2010; Soil Survey Staff, 2017). Therefore, because depth to permafrost is a dynamic soil property, permafrost-affected soils, by definition, are a dynamic taxonomic entity (Ping, 2013b). Thus, the ongoing degradation of NSP in Alaska due to climatic change will have a widespread impact on permafrost-affected soil classification at the highest levels, and understanding taxonomic change in permafrost-affected soils is therefore important for the planning, ultimate longevity, and usefulness of existing, in-progress, and future soil surveys in Alaska.

Moreover, due to the imminent 21st-century loss of NSP across the circumpolar region (Guo & Wang, 2016), some or all permafrost-affected soil taxa may become threatened or extinct (Drohan & Farnham, 2006). Because permafrost-affected soils and NSP are critical for ecosystem functioning in cold regions and are of extremely high scientific interest, they also warrant investigation into the potential extent of their loss and subsequent implications for their recognition as rare or threatened soils (Drohan & Farnham, 2006).

The objective of this study was therefore to generate spatially explicit estimates of the potential extent of major permafrost-affected soil classes (the Gelisol order and Histel, Orthel, and Turbel suborders) in US Soil Taxonomy across the state of Alaska throughout the 21st century due to NSP loss. We accomplished this objective by integrating a suite of published models of active layer thickness and NSP change from 2000 to 2099 under low (Special Report on Emissions Scenario [SRES] B1, Representative Concentration Pathway [RCP]4.5), moderate (SRES A1B),

TABLE 1 Near-surface permafrost (NSP) input data sources, references, emission scenarios, temporal span, modeled properties, and spatial resolutions.

Data source	Future change scenario	Year range	Modeled property	Derived diagnostic feature	Spatial resolution
Pastick et al., 2015	SRES: A2, A1B, B1	2000–2009, 2050–2059, 2090–2099	Probability of NSP within 1 m of soil surface (presence/absence)	Permafrost within 1 m	30 m
Jafarov et al., 2012	SRES: A1B	2000–2009, 2050–2059, 2090–2099	Active layer thickness to 2 m	Permafrost within 2 m	2 km
Aalto et al., 2018	RCP: 4.5, 8.5	2000–2014, 2041–2060, 2061–2080	Active layer thickness to 2 m	Permafrost within 2 m	30 arc seconds (~1 km)
Yi & Kimball, 2020	N/A	2000–2015	Active layer thickness to 2 m	Permafrost within 2 m	1 km
Genet et al., 2016	N/A	2000–2015	Active layer thickness to 2 m	Permafrost within 2 m	1 km

Abbreviations: N/A, not available; RCP, Representative Concentration Pathway; SRES, Special Report on Emissions Scenario.

and high (SRES A2, RCP 8.5) emission scenarios with the current distribution of Gelisol orders and suborders across the state of Alaska (STATSGO2; Soil Survey Staff, 2022b). These spatially explicit estimates of Gelisol order and suborder taxonomic change can then be integrated into the design of future mapping, re-mapping, or re-correlation efforts and used to assess the future status of Gelisol taxa as rare or threatened soils in the United States.

2 | MATERIALS AND METHODS

2.1 | Estimates of 21st-century near-surface permafrost extent

2.1.1 | Baseline (early-century) estimates of near-surface permafrost extent

We utilized five different data sources to estimate early 21st-century "baseline" NSP extent across Alaska (Table 1). Pastick et al. (2015)—referred to as "Pastick"—utilized machine learning (boosted regression tree) to generate binary presence/absence probabilities for NSP within 1 m of the soil surface at 30-m resolution on a statewide basis using 17,000 mid-late season (post-July) observations from 1990 to 2013 of NSP presence or absence. Aalto et al. (2018)—referred to as "Aalto"—utilized 303 site-specific active layer depth datasets in combination with adjusted WorldClim data (Hijmans et al., 2005), digital elevation model (DEM)-derived incoming solar radiation estimates, and soil organic carbon (SOC) concentrations (Hengl et al., 2014) as inputs to multiple statistical modeling and machine learning (random forest) approaches to generate active layer thickness estimates to a depth of 2 m at 30 arc second resolution for the entire northern circumpolar region. Yi and Kimball (2020)—referred to as "Yi"—utilized remote sensing data from Moderate Resolution Imaging Spectroradiometer (MODIS) land surface temperature and snow cover extent, and Soil Moisture Active and Passive satellite data from 2001 to 2015 to drive a soil process model (Yi et al., 2015) at 1-km resolution across the state of Alaska to estimate active layer thickness based on the soil depth at which the OC threshold is crossed (Yi et al., 2018). For the Yi dataset, the average modeled active layer thickness from 2001 to 2015 was utilized as our baseline input (Yi & Kimball, 2020). Jafarov et al. (2012)—referred to as "GIPL" (Geophysical Institute Permafrost Laboratory)—utilized the process-based GIPL2-MPI numerical model (a one-dimensional numerical heat flow model that simulates active-layer thickness and soil temperatures) driven by the Scenarios Network for Alaska Planning (SNAP) dataset (Walsh et al., 2008), downscaled to 2 km using PRISM climate data (PRISM Climate Group at Oregon State University, n.d.) and modified by soil types and organic layer thickness. Finally, Genet et al. (2016) generated statewide predictions of active layer thickness using the DOS-TEM model—referred to as "DOS-TEM"—a numerical model that simulates biophysical processes in permafrostaffected ecosystems (Genet et al., 2016). Together, these five datasets represent independently derived estimates of early 21st-century statewide NSP distribution with an aggregate temporal resolution (based on input data) of 2000-2015 (Table 1).

Each of these data sources were converted to binary NSP presence/absence rasters by "hardening" the raw values either by $\geq 50\%$ NSP probability (in the case of the Pastick dataset), or by assigning all raster cells that had active layer thickness values of 2 m or less (in the case of the Yi, DOS-TEM, GIPL, and Aalto datasets) a value of 1 and all other cells a value of 0 (Figure 1). It is important to note that although 50% thresholds are often used to arbitrarily "harden" probabilities into binary presence-absence information, in the case of the

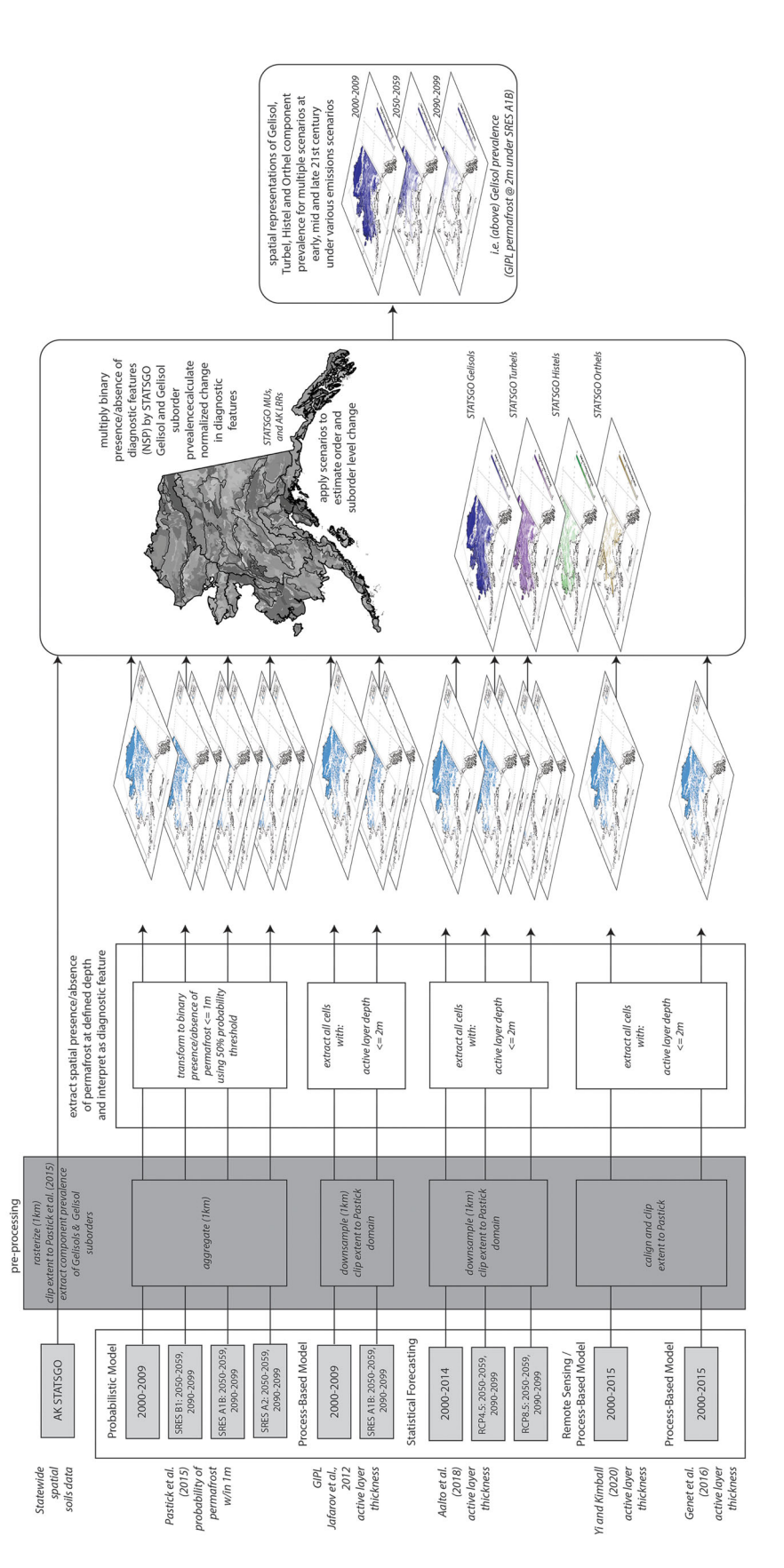


FIGURE 1 General processing workflow and spatial operations for input datasets to produce derived estimates of Gelisol order and suborder taxa distributions.

Pastick dataset this was the threshold that also maximized correspondence between historic field observations and model estimates of the presence-absence of permafrost at 1-m depth, which is described in the original study (Pastick et al., 2015). Both the Jafarov et al. (2012) and Aalto et al. (2018) datasets were simply converted to binary format for any cells meeting the criteria of active layer thickness ≤2.0 m because there were no associated probabilities assigned to the active layer thickness estimates that were represented on a continuous scale.

2.1.2 | Mid- to late century estimates of near-surface permafrost extent under varying emissions scenarios

Three of the five data sources utilized to estimate earlycentury baseline NSP extent also projected corresponding mid- and late 21st-century NSP extent estimates under differing emissions scenarios (Table 1). Pastick et al. (2015) utilized SNAP (Walsh et al., 2008) global climate model (GCM) ensemble climate projections for SRES B1 (low emissions), A1B (moderate emissions), and A2 (high emissions) at mid- (2050-2059) and late (2090-2099) 21st-century time periods. The SNAP projections were produced using an identical ensemble of outputs from the five top ranked GCMs from the Fourth Assessment Report of the Intergovernmental Panel on Climate Change (Walsh et al., 2008). Jafarov et al. (2012) also utilized SNAP GCM ensemble climate projections but for SRES A1B only, at mid- (2050-2059) and late (2090-2099) 21st-century time periods. Finally, Aalto et al. (2018) utilized Coupled Model Intercomparison Project (CMIP) ensemble projections (Moss et al., 2010) for three RCP scenarios RCP 2.6 (low emissions), RCP 4.5 (moderate emissions), and RCP 8.5 (high emissions), at mid-(2040–2060) and late (2061–2080) century time periods.

Several of the SRES and RCP scenarios are broadly analogous, and therefore for the purposes of our analysis, we grouped them into low emission (B1 ~540 ppm 2100; RCP $4.5 \sim 550$ ppm 2100), moderate emission (A1B ~ 710 ppm 2100), and high emission (A2 ~860 ppm 2100; RCP 8.5 ~940 ppm 2100) pathways (Snover et al., 2013). Note that although Aalto et al. (2018) utilized the RCP 2.6 scenario (an aggressive mitigation scenario with 420 ppm by 2100), we did not use this scenario in our analysis here because there is no corresponding SRES scenario with the same aggressive mitigation. Similarly, the RCP scenario that corresponds most closely to SRES A1B is RCP 6.0 (~670 ppm 2100); however, this was not a scenario utilized by Aalto et al. (2018). Additionally, we grouped the projected time periods into two major categories of mid-century (2040-2060) and late century (2061-2099) based on the time periods spanning the projections of the original data sources. Therefore, the two mid- and late-century projection time periods, in combination with early-century baseline estimates (2000–2015) for these three datasets (early-, mid-, and late century), along with three emissions categories (low, moderate, and high emissions) each containing two independent estimates of NSP extent, resulted in a set of nine potential NSP extent projections across all time periods and emissions categories (Figures S1–S4).

2.2 | Permafrost-affected soil taxa definitions, prevalence, and extent

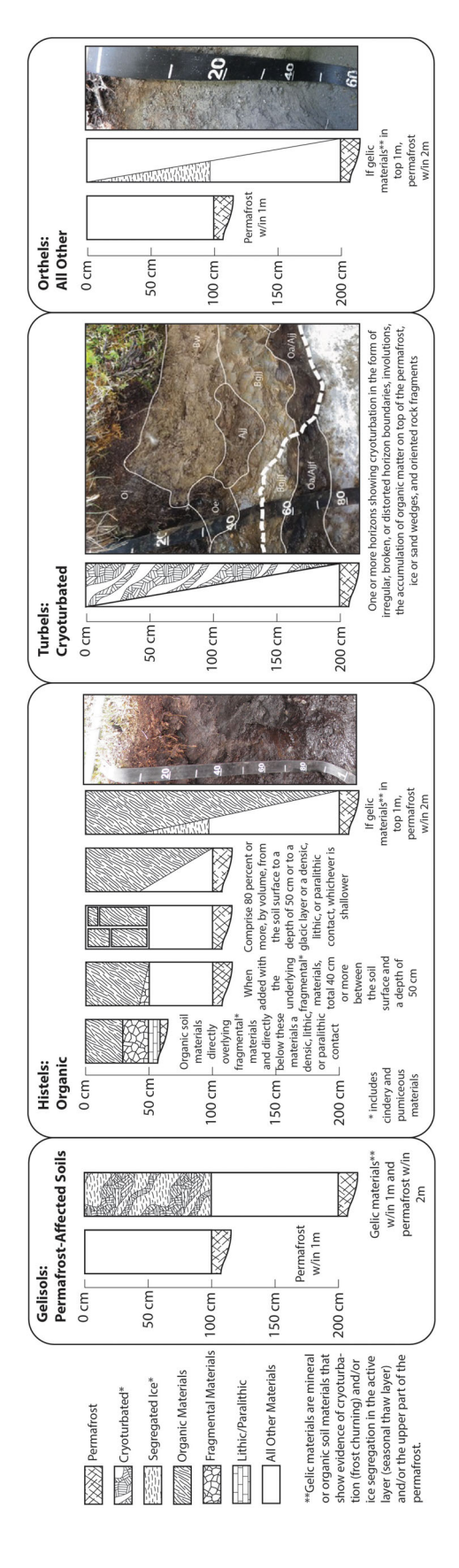
2.2.1 | Permafrost-affected soil taxa criteria and definitions in US Soil Taxonomy

We focused our analysis on permafrost-affected soil taxa defined at the order and suborder level in US Soil Taxonomy: the Gelisol order and three corresponding suborders. To be classified as a Gelisol in US Soil Taxonomy, a soil must have permafrost within 1 m of the soil surface or within 2 m of the soil surface if the soil contains gelic materials within 1 m of the soil surface (Soil Survey Staff, 2022a; Figure 2). The gelic material concept in US Soil Taxonomy was designed to provide quantitative and objective criteria to identify morphological markers of cryogenic processes (Bockheim & Tarnocai, 1998), which may include cryoturbation (in the form of irregular/broken horizons, organic matter accumulation near the permafrost, oriented rock fragments) and/or evidence of ice segregation (in the form of platy or blocky cryogenic structures in the active layer or ice lenses and vein ice in the permafrost) among other characteristics (Ahrens et al., 2004; Soil Survey Staff, 2022a).

Orthels, Turbels, and Histels are the three recognized Gelisol suborders in the US taxonomic system (Soil Survey Staff, 2022a). Orthels are non-cryoturbated mineral soils with thin organic materials at the surface; Turbels are cryoturbated mineral soils and are the most widely distributed Gelisol suborder in the state of Alaska and the northern circumpolar region (Soil Survey Staff, 2022a; Tarnocai et al., 2002), and Histels are organic soils characterized by greater than 40 cm of organic surface materials in most cases (Soil Survey Staff, 2022a). The extent and prevalence of these permafrost-affected soil classes across Alaska are represented in both the gridded National Soil Survey Geographic Database (gNATSGO; Soil Survey Staff, 2022c) and the Alaska State Soil Geographic (STATSGO2) dataset (Soil Survey Staff, 2022b).

2.2.2 | gNATSGO

The gridded National Soil Survey Geographic Database (gNATSGO) product for Alaska is delivered as a composite raster database that combines Soil Survey Geographic



Graphical depiction of Gelisol, Histel, Turbel, and Orthel classification criteria in US Soil Taxonomy (Soil Survey Staff, 2022a). FIGURE 2

Database (SSURGO)-compliant data (mapped at scales ranging from 1:12,000 to 1:63,360) where it is available (Figure S5) and the Alaska State Soil Geographic (STATSGO2) dataset to provide seamless coverage (Soil Survey Staff, 2022c) at 10-m resolution. Detailed soil survey data for Alaska in the gNATSGO dataset, as would be provided by SSURGO, are currently only available for less than 20% of the state of Alaska (Figure S5). Due to the limited spatial extent of SSURGO data in the gNATSGO dataset, gNATSGO was used in a limited manner as an alignment template (see Section 2.3.2) and as the primary source of SSURGO-compliant data to compare and contextualize permafrost-affected soil taxa distributions and extent from STATSGO2 within currently published SSURGO-compliant survey areas (Section 2.2.3, Figure S5).

2.2.3 | STATSGO2

We utilized the Alaska State Soil Geographic (STATSGO2) dataset (Soil Survey Staff, 2022b)—the only currently available statewide soils dataset for Alaska—as a representation of the spatial distribution and prevalence of permafrost-affected soil taxa. The STATSGO2 dataset is currently delivered as a vector dataset, with polygons and tabular data linked through unique map unit key (*mukey*) values (Soil Survey Staff, 2022c).

The Alaska STATSGO2 dataset is mapped at a smaller scale (1:500,000) than the STATSGO2 dataset for the contiguous United States (1:250.000), with a standard minimum delineated area of 2500 ha (25 km²), except in the case of off-shore islands, which may be smaller (Clark, 2012). STATSGO2 was designed for regional, multi-county, river basin, or statewide analysis and thus is appropriate for the analysis scale applied in this study. Alaska STATSGO2 map units were manually delineated based on existing soil surveys, landforms, life zones, and existing vegetation types; and delineations were field verified with a limited dataset of 207 point and transect data (Clark, 2012). There are 2252 map unit delineations in the Alaska STATSGO2 map—covering an area of 1,507,830 km², the mean delineation size is 669 km², the median delineation size is 26 km², the minimum delineation size is less than 1 km² (offshore islands), and the maximum delineation size is 63,312 km². Ignoring offshore island delineations in STATSGO2, the mean and median delineation sizes for STATSGO polygons (1131) across AK are 1330 and 404 km², respectively.

Every unique map unit has a unique key (mukey), which is associated with a number of components (entities which are classified to the great group level in the Alaska STATSGO2 dataset) for the map unit in the STATSGO2 and gNATSGO tabular data. In the AK STATSGO2 dataset, the average number of components per map unit is 6.4 ± 3.3 , with a

minimum of 1 and maximum of 18. Unique soil components (classified to the great group level in US Soil Taxonomy) are assigned, with representative percentages (*comp pct_r*), to every delineated map unit in the Alaska STATSGO2 dataset. Minimum and maximum (low and high) map unit component percentages—typically assigned in the SSURGO database—are not available in the Alaska STATSGO2 dataset. The component soil classes assigned to each delineated map unit and their properties are contained in tabular form in the component table of STATSGO2. There are 260 unique map units and 1664 unique components in the AK STATSGO database.

2.2.4 | Calculation of permafrost-affected soil taxa prevalence in STATSGO and gNATSGO

The distribution and prevalence of each permafrost-affected soil taxon to the suborder level (the Gelisol order and the Turbel, Histel, and Orthel suborders) were calculated for each map unit in the STATSGO and gNATSGO datasets map unit by utilizing the STATSGO and gNATSGO component tables. The prevalence (prev, or proportion of the raster cell) of each permafrost-affected soil taxa y in the map unit can be calculated as the sum of *comp* pct_r) for all components assigned to the map unit matching taxon. The representative percentages of components in each unique map unit must add up to 100%. However, due to the presence of non-soil components in some STATSGO2 map units ("rock outcrop and rubbleland," "riverwash," "water," "dunes," "tidal flats," "cinderland and lava flows," "beaches, gravelly," "ice and permanent snowfields," "Urban Land," and "cinder land", which are poorly spatially resolved and not delineated), we used the Pastick dataset as the single best spatial representation of the soil and non-soil domain areas across the state of Alaska (see Section 2.3.2, Figure S6). The raw prevalence values for taxon y in each map unit were subsequently normalized by soil component percentages (Equation 1). This avoids double counting that would occur if the soil domain of Pastick was utilized, but permafrost-affected soil taxa prevalence was not normalized by soil component prevalence. Therefore, the prevalence of each permafrost-affected soil taxa in our baseline STATSGO2 data representation was calculated as:

if
$$j \ge 1$$
: $\operatorname{prev}_{y,\text{soil}} = \frac{\sum_{k=1}^{N_y} o_r(comp \ pct_{r,y})}{\sum_{j=1}^{N_{\text{soil}}}(comp \ pct_{r,\text{soil}})}$, (1)
if $j = 0$: $\operatorname{prev}_{y,\text{soil}} = 0$

where j is the number of soil components in the map unit, prev_{y,soil} is the prevalence of taxon y in the map unit for soil components only. comp $pct_{r,y}$ is the representative percentage of a single component matching taxon y. Note that the numerator on the right hand of the equation is summed for all matching components k to N_y , where k = 1 and $N_y =$ the

total number of matching components for multiple matching components, $k = N_y = 1$ in the case of a single matching component, or $k = N_y = 0$ in the case of no matching components. Conversely, the denominator on the right hand of the equation is summed for all soil components j to $N_{\rm soil}$, where j = 1 and $N_{\rm soil}$ = the total number of soil components. If there are no soil components assigned to a map unit ($j = N_{\rm soil} = 0$), then prev_{y,soil} is set to 0.

2.2.5 | Alaskan land resource regions as appropriate units of analysis

Land resource regions (LRRs) are defined by a unique set of topographic, landscape, hydrologic, resource concerns, resource uses and human considerations affecting use and soil and water conservation treatment needs (USDA-NRCS, 2022). Currently, the five LRRs in Alaska are Southern Alaska (LRR W1), comprising much of the south central and south-eastern portions of the state—south of the Alaska Range and Wrangell Mountains, including the area surrounding the Cook Inlet, the Kodiak Archipelago, the Alexander Archipelago, and the eastern portion of the Alaskan Peninsula; Aleutian Alaska (LRR W2) including the Aleutian Archipelago and the western portion of the Alaskan Peninsula; Western Alaska (LRR X2) containing the Yukon-Kuskokwim Delta, Nulato Hills, portions of the northern Alaska Peninsula, and the southern Seward Peninsula; Interior Alaska (LRR X1) containing most of the central and eastern portions of the state north of the Alaska Range and south of the Brooks Range, including the Copper River Basin to the south and Yukon Flats to the east; and Northern Alaska (LRR Y) comprising the northern Seward Peninsula and north of the Brooks Range to the Beaufort Sea (Figure \$7).

We chose to utilize LRRs as our sub-state spatial unit of analysis in order to (1) capture taxonomic change across land-scape units that are relevant to soil survey and ecological realities and (2) because LRRs are of reasonable size given the mapping scale and limitations of the STATSGO2 dataset. The median STATSGO2 delineation size (404 km²) results in an average minimum of 51 delineation units in the smallest LRR (X2). Therefore, given the scale of mapping for the Alaska STATSGO2 dataset, LRRs are appropriate for understanding large sub-state geographic trends.

2.3 | Spatial domain extent and spatial and temporal resolution

2.3.1 | Spatial resolution and data pre-processing

We chose to utilize a 1-km spatial resolution in this analysis as a reasonable compromise between the resolutions of the input datasets (ranging from 30 m (Pastick et al.,

2015) to 2 km (Jafarov et al., 2012), as well as the scale for use of the STATSGO2 dataset (Section 2.2.3; Figure 1). Because the gNATSGO product covers the entire spatial extent of the state of Alaska, and because it contained out-ofthe-box 10-m resolution, we first aggregated the gNATSGO dataset to 1-km resolution using a nearest neighbor algorithm implemented in the terra::resample function in R. All other raster input datasets were resampled (aligned and aggregated or downscaled) to the 1-km gNATSGO dataset using the terra::resample algorithm in R, using nearest neighbor resampling for all categorical and binary layers (NSP input datasets) and cubic convolution resampling for all continuous layers (STATSGO and gNATSGO permafrost-affected soil taxa prevalence; Figure 1). Because the raw form of the STATSGO2 dataset is a vector, it was rasterized and resampled to match the aggregated 1-km AK gNATSGO dataset prior to additional analysis (Figure 1).

2.3.2 | Analysis domain and spatial extent

We utilized the extent of the Pastick et al. (2015) dataset (which excludes St. Lawrence and St. Matthew islands in the northern Bering Sea and the Aleutian islands west of Unalaska) as our analysis domain. This domain is 1,488,816 km² in total, with 252,761 km² of non-soil area (surface water, ice, rock, and urban areas) and 1,236,055 km² of soil area. This domain was chosen for several reasons: (1) the Pastick et al. (2015) dataset in raw form was the smallest extent and therefore all other datasets overlapped with it—the same was not true of any other datasets; (2) it is superior to the other extents for our display purposes, focusing on permafrostaffected soils in mainland Alaska; (3) the western Aleutian islands and St. Matthew and St. Lawrence have essentially no NSP occurrence and comprise relatively minor overall land area. Therefore, the exclusion of these portions of Alaska in our analysis domain has minimal impact on our results. Additionally, we utilized the aggregated 1-km Pastick et al. (2015) dataset to mask all non-soil cells from our analysis domain (Figure S6). The Pastick et al. (2015) dataset is one of the highest quality statewide datasets available representing the spatial extent of non-soil land cover (i.e. rock, ice, water, and urban lands), as the boosted regression tree algorithms used in the production of this dataset specifically predicted these land cover types with high accuracy (Pastick et al., 2015). This non-soil masking integrates with our calculation of permafrost-affected soil taxon prevalence from gNATSGO and STATSGO2 on a soil component basis only, as including non-soil components in these prevalence calculations yields anomalous results for some regions due to the high prevalence of small water bodies that are not well spatially represented in the STATSGO2 database.

2.4 | Generating dataset-specific baseline and mid-late century estimates of permafrost-affected soil taxa extent and prevalence

We utilized the 1-km aggregated STATSGO2 soil domain (Section 2.3.2) as the statewide source of taxon prevalence information. Gelisols account for 45% (556,833 km²) of the state soil domain (1,236,055 km²) and are unequally distributed between LRRs in Alaska (Figure 3, Table 2). Among LRRs, Interior Alaska (X1) contains the largest area of Gelisols (264,665 km²), while (with the exception of Aleutian Alaska [W2] at 0 km² of Gelisols), Southern Alaska (W1) has the smallest area of Gelisols at 98 km² (Table 2). Northern Alaska (Y) contains the highest proportion of Gelisols as a percent of land area (73.5%; Table 2). Orthels (45%) and Turbels (44%) account for the vast majority of Gelisols in the Alaska followed by Histels (11%; Table 2, Figure 3). Interior Alaska (X1) contains the greatest extent of Orthels (173,210 km²) among all LRRs (Table S1), while Turbels are dominant in Northern Alaska (140,262 km²) (Table 2, Figure 3). Histels are nearly evenly distributed between Interior (20,046 km²) and Northern (29,648) Alaska (Table 2, Figure 3).

A permafrost-affected soil taxon prevalence raster was generated from each NSP input dataset (all five early century and three mid- and late-century datasets) by multiplying the STATSGO taxon prevalence raster by each binary NSP presence/absence raster using Equation (2) as follows:

$$pre \ v_{y,soil,x} = prev_{y,soil} \times nsp_{binary,x},$$
 (2)

where $prev_{y,x}$ is the prevalence of permafrost-affected soil taxon y for NSP dataset x, $prev_{y,\text{soil}}$ is the prevalence of taxon y among all soil components derived from the STATSGO2 dataset as described in Equation (1), and $nsp_{binary,x}$ is the binary NSP value (1 for present and 0 for absent) from each of the baseline, mid-, and late century NSP extent rasters (Table 1, Section 2.2.4). This approach results in estimates of permafrost-affected soil taxon prevalence, which can then can be used to generate permafrost-affected soil taxa extent for each dataset and scenario (by summation).

2.5 | Spatial operations and statistical analysis

All spatial operations described in the methods were performed in R with the exception of export of the gNATSGO dataset to 1 km (as gNATSGO is delivered as a proprietary .gdb format and therefore must be initially manipulated in ArcGIS prior to exporting as a .tif). Spatial operations and analysis were performed in the terra package in R (Hijmans

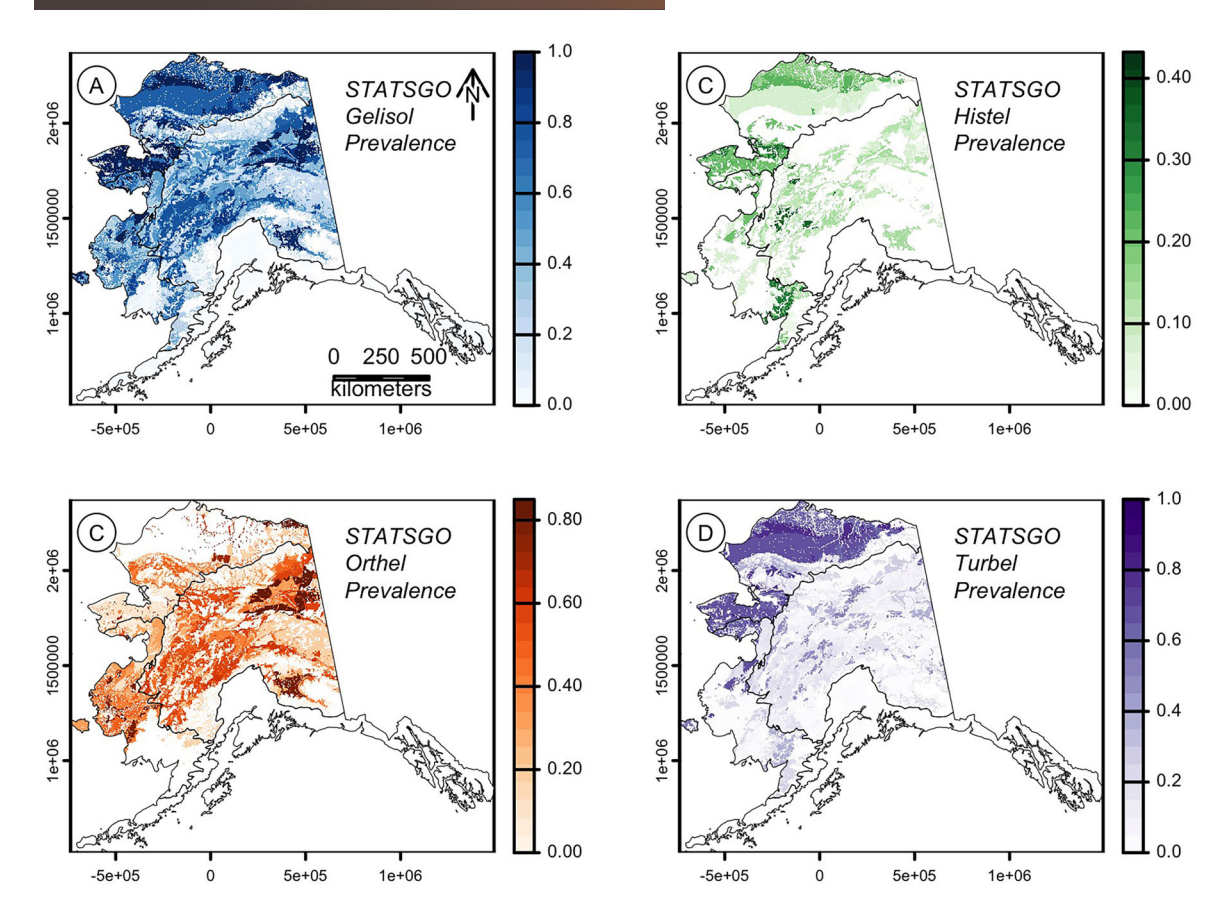


FIGURE 3 Prevalence (component weighted proportion of map unit, normalized to soil components) of (A) Gelisols, (B) Histels, (C) Orthels, and (D) Turbels across the state of Alaska in the STATSGO2 dataset (Soil Survey Staff, 2022a).

TABLE 2 General areas of Alaskan land resource region (LRR) total and soil domains included in this analysis (upper); areas of Gelisol order and suborder taxa by LRR—percentages following numbers refer to the percent of the LRR soil domain occupied by that taxonomic class (middle); estimated Gelisol area by LRR, derived by multiplying binary near-surface permafrost (NSP) rasters by STATSGO Gelisol presence (Figure 1, Equation 2).

	Land resource re							
Area (km²)	Southern (W1)	Aleutian (W2)	Interior (X1)	Western (X2)	Northern (Y)	Total		
	General							
Domain	275,042	148	665,522	223,206	324,898	1,488,816		
Soil	176,503	123	583,670	195,059	280,700	1,236,055		
	Permafrost-affected soil classes (STATSGO)							
Orthels	11 (<1%)	0	173,210 (29.7%)	44,062 (22.6%)	36,291 (12.9%)	253,574 (20.5%)		
Turbels	76 (<1%)	0	71,410 (12.2%)	31,346 (16.1%)	140,262 (50.0%)	243,094 (19.7%)		
Histels	11 (<1%)	0	20,046 (3.4%)	10,461 (5.4%)	29,648 (10.6%)	60,166 (4.9%)		
Gelisols	98 (<1%)	0	264,665 (45.3%)	85,869 (44.0%)	206,201 (73.5%)	556,833 (45.1%)		
	Baseline Gelisol prevalence estimates							
Yi	10	0	169,275	12,732	195,795	377,812		
Aalto	14	0	176,553	24,108	205,389	406,064		
DOS-TEM	3	0	115,146	10,156	153,010	278,315		
GIPL	14	0	206,306	42,860	206,029	455,209		
Pastick	3	0	123,846	22,865	186,087	332,801		
Average ± SD	9 ± 6	0	$158,225 \pm 38,104$	$22,544 \pm 12,894$	189,262 ± 21,841	$370,040 \pm 67,845$		

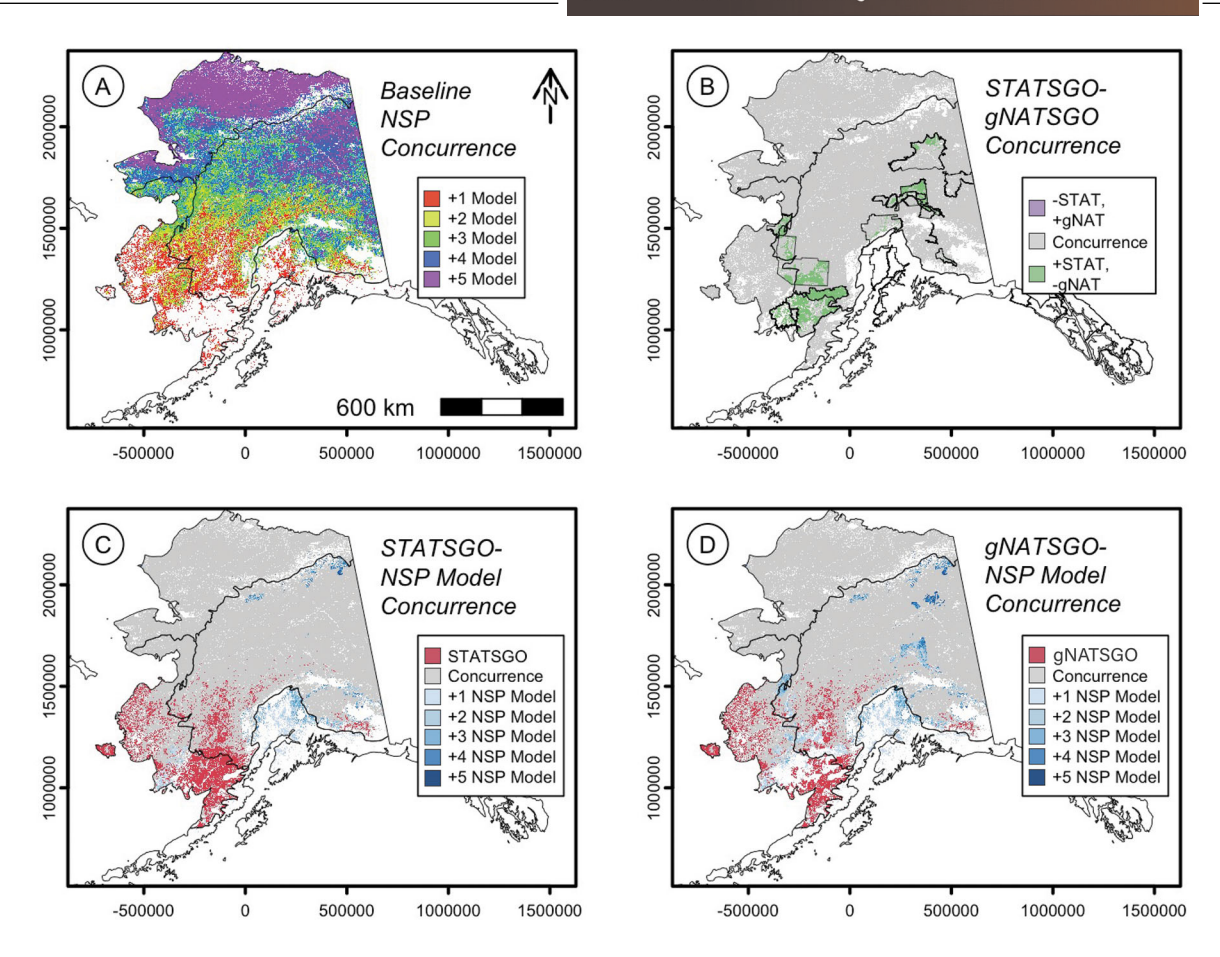


FIGURE 4 Concurrence of baseline dataset near-surface permafrost (NSP) binary presence/absence predictions and Gelisol presence across the state of Alaska. (A) Number of models predicting NSP presence by 1-km raster cell, (B) differences in 1-km raster cells containing Gelisols (regardless of prevalence) between the STATSGO dataset and the gNATSGO dataset—the gNATSGO dataset contains SSURGO data for select completed survey areas (outlined in black); (C) concurrence between STATSGO Gelisol presence and baseline NSP dataset binary presence/absence—areas in red have STATSGO Gelisols that are not predicted by any NSP models, areas in gray have Gelisols predicted by STATSGO and at least one baseline model predicting NSP presence, and areas in blue have no Gelisols predicted by STATSGO but NSP predicted by at least one or more baseline datasets; (D) same as (C), but for the gNATSGO dataset.

et al., 2023; Team, R Core, 2023). Detailed source code files containing scripts that implement these operations as well as the generation of all figures and tables in the manuscript can be found in the Supporting Information and at the GitHub and UMN DRUM repositories for this study (https://github.com/jelinski-lab-pedology/M007-jelinski-gelisol-change-ak).

3 | RESULTS

3.1 | Early 21st-century baseline estimates of NSP and Gelisol extent

The five different data sources utilized to estimate early 21st-century "baseline" NSP and Gelisol extents in Alaska varied in their predictions and were characterized by important differences relative to STATSGO2 (Figure 4, Table S1). The binary GIPL model resulted in the largest extent of NSP

in the baseline situation (825,666 km²), whereas the binary DOS-TEM model predicted the lowest extent of NSP in Alaska (489,427 km²), with an average predicted extent of $641,896 \pm 145,699 \text{ km}^2$ (Table S1). Concurrence between these five independent models varied by LRR, with the greatest variability between models in Southern and Western Alaska (Figure 4). Predicted baseline binary NSP extents among these five datasets were most uncertain in Southern $(9391 \pm 5126, \text{ coefficient of variation (CV)} = 55\%)$ and Western Alaska (41,514 \pm 23,520 km², CV = 57%) and least uncertain in Northern Alaska (252,072 ± 33,693 km2, CV = 13%), with the greatest absolute aerial uncertainty in Interior Alaska $(338,918 \pm 94,230 \text{ km}^2, \text{CV} = 28\%)$ (Figure 4, Table S1). Note that these binary NSP presence/absence aerial extents are much higher than actual Gelisol extents because they assume an entire pixel contains NSP. This is why permafrost-affected soil taxa prevalence from STATSGO2 provides a critical integration with NSP predictions, as it

provides aerial estimates permafrost-affected soil prevalence at the sub-grid scale (Figure 1, Equation 1).

Because STATSGO aerial coverage of Gelisols was more extensive than any single NSP model estimate, particularly in Southern and Western Alaska (Figure 4C), all baseline Gelisol extent estimates (370,040 \pm 67,845 km²) were lower than that from STATSGO dataset (556,833 km²). The fewest discrepancies between STATSGO Gelisol extent and baseline Gelisol extent estimates occurred in Northern Alaska, where NSP estimates were most certain (Figure 4A,C). There were several small areas in Southern and Interior Alaska where a limited number of datasets predicted NSP that was not covered in STATSGO; however, these were extremely limited in extent (Figure 4C).

Assessing the extent to which STATSGO may over or under estimate Gelisol extent can be accomplished by comparing STATSGO Gelisol estimates with gNATSGO Gelisol estimates for the limited survey areas where SSURGO quality data are available (Figure S5, Figure 4B). Most current SSURGO coverage occurs in Interior and Southern Alaska (Figure S5, Figure 4B). Among the 21 SSURGO survey areas, total Gelisol extents are predominantly lower than STATSGO estimates (Figures S8–S28, Figure 4B); however, in two survey areas (Denali National Park and Preserve [Figure S11] and Yukon-Charley National Park and Preserve [Figure S27]), SSURGO level mapping resulted in no-change (Denali) or increased Gelisol extents (Yukon-Charley).

Although there is reasonable concurrence between SSURGO Gelisol extent and NSP baseline predictions, there are instances where SSURGO level mapping contains significantly greater (Bristol Bay) or lower (North Star, Togiak) Gelisol extent than any of the NSP baseline scenarios (Figures S8–S28). Across all SSURGO survey areas, NSP extents from the GIPL and Pastick models were most closely correlated to Gelisol extent (0.91 and 0.89, p < 0.01, Pearson's correlation test), followed by Yi (0.85) and Aalto (0.77). Notably, the GIPL statewide baseline Gelisol estimates are the highest among all datasets (455,209 km²) and closest to the STATSGO Gelisol estimate (556,833 km²). Therefore, based on the differences between STATSGO and SSURGO, as well as the differences between NSP predictions and STATSGO (Figure 4), we assume that the STATSGO represents an upper bound on Gelisol extent across the state of Alaska.

3.2 | Estimates of mid- and late century Gelisol taxonomic change

Low emission scenarios (RCP 4.5, SRES B1) resulted in significant changes in Gelisol extent across all LRRs. However, the Aalto low emission models resulted in significantly greater changes in Gelisol extent in Interior (-72%), Western (-98%), and Northern Alaska (-23%) by mid-century

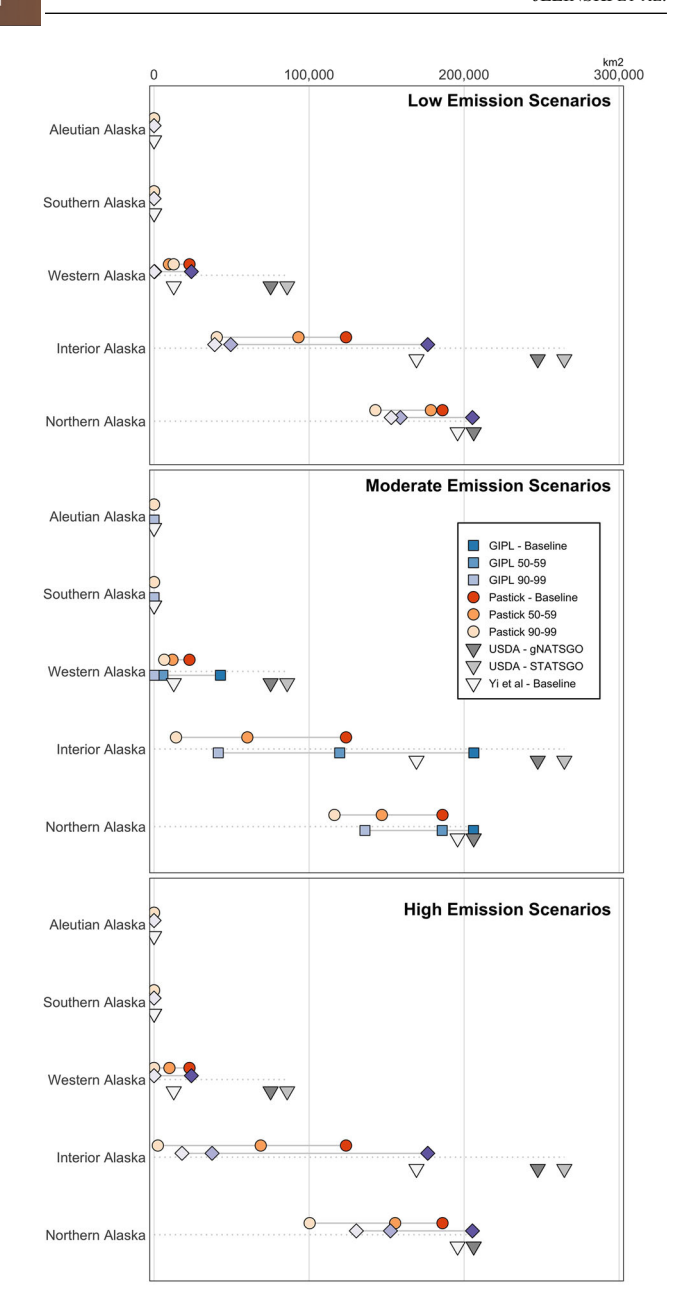


FIGURE 5 Dumbbell plot of Gelisol area by Alaska land resource region (LRR) for STATSGO, gNASTGO, Baseline datasets, and under low (Special Report on Emissions Scenario [SRES] B1, Representative Concentration Pathway [RCP] 4.5), moderate (SRES A1B), and high (SRES A2, RCP 8.5) emission scenarios.

than the Pastick model (-24%, -58%, and -4%, respectively, Table S2, Figures 5 and 6), and thus mid-century loss uncertainty was the greatest in Western and Interior Alaska. Late century loss predictions were much more similar between Aalto and Pastick for Interior (-78% and -67%, respectively) and Northern Alaska (-26% and -23%, respectively; Table S2). Pastick and Aalto shared similar early century Gelisols extent predictions in Western Alaska (22,865 and 24,108 km², respectively; Table S2, Figures 5 and 6). However, future losses in Western Alaska diverged significantly, with Aalto predicting nearly complete Gelisol loss (-98%)

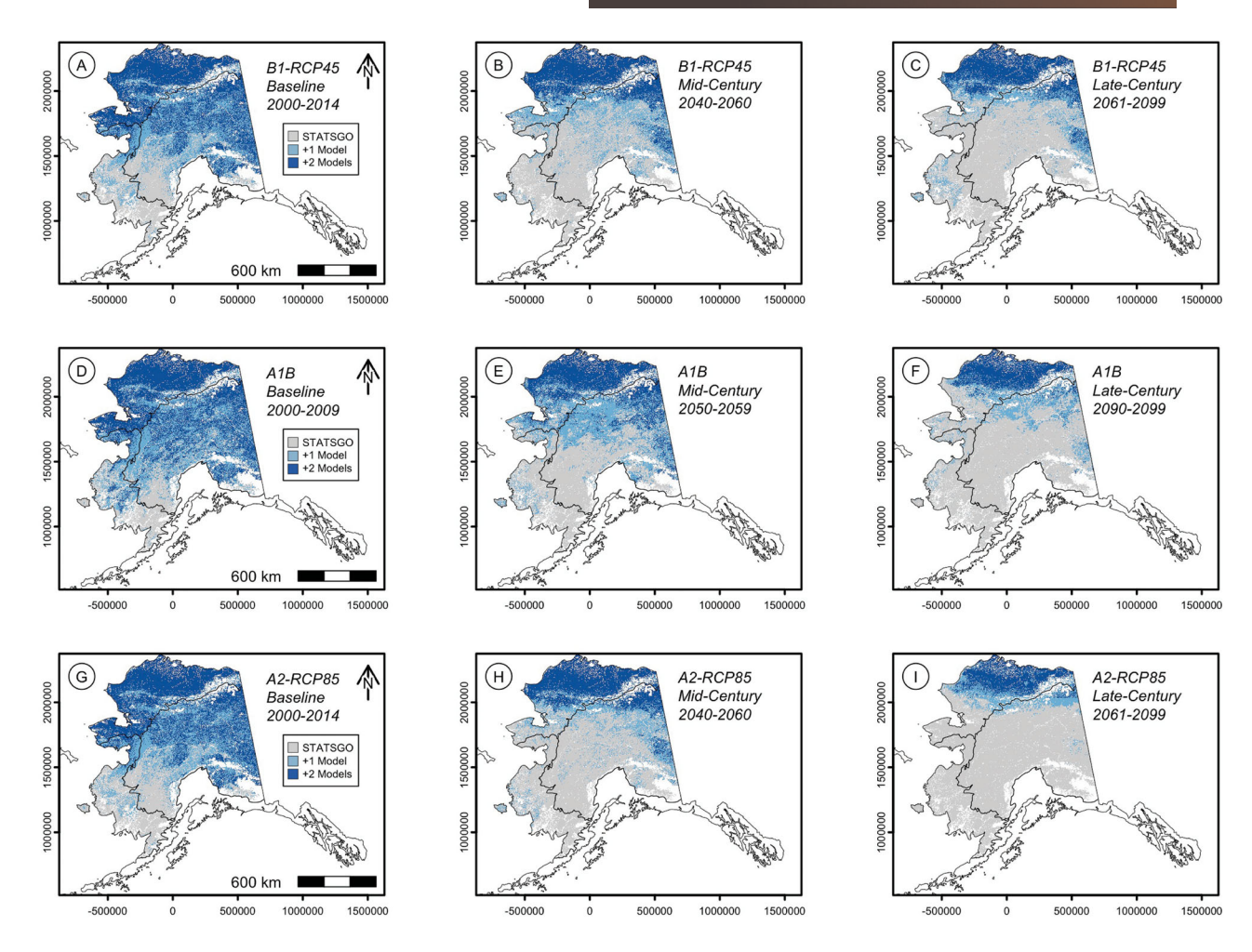


FIGURE 6 Binary representation of 1-km raster cells that contain Gelisols for early 21st-century baseline scenarios, and under low (Special Report on Emissions Scenario [SRES] B1, Representative Concentration Pathway [RCP] 4.5), moderate (SRES A1B), and high (SRES A2, RCP 8.5) emission scenarios. The gray areas contain Gelisols in the STATSGO dataset, while areas in blue have either one or two near-surface permafrost (NSP) models predicting Gelisol presence (regardless of prevalence). Note that there are exactly two data sources in each emissions scenario category (Section 2.1.2).

by mid-century and -99% by late century), while Pastick predicted more moderate losses (-45% by late century).

Mid emission scenarios (SRES A1B) also resulted in significant change in Gelisol extent across all LRRs. Similar to the low emission scenarios, scenarios differed most widely in Western Alaska, where mid-century losses ranged from –48% (Pastick) to –87% (GIPL). Mid-century loss predictions in Northern Alaska were much less variable (–10% to 21%) across models. However, regardless of the model, absolute Gelisol losses by mid-century in Interior Alaska were the greatest among all LRRs (–63,639 km²; Pastick to –89,555 km²; GIPL). Late century relative changes were less variable between models and the greatest for both Interior (–80% and –89%) and Western (–71% and –99%) Alaska (Table S3, Figures 5 and 6). Predicted late century Gelisol loss in Northern Alaska was most similar and less extensive than other LRRs (–37% and –34%; Table S3, Figures 5 and 6).

High emissions scenarios exhibited the greatest variability between models but exhibited similar patterns (with

more extensive losses) as low and mid emissions scenarios. Mid-century Gelisol losses were extremely variable between models for Interior (-44% and -79%) and Western Alaska (-56% to -99%; Table S2, Figures 5 and 6). Most critically, late century model predictions resulted in nearly complete loss of Gelisols in Southern (100%), Interior (-90% to -98%), and Western Alaska (-100%). Only Northern Alaska Gelisols are less susceptible to loss in the high emissions scenarios (-36% to -47%; Table S4, Figures 5 and 6).

Due to the uneven distribution of Gelisol suborders across the state of Alaska (Figure 3), Gelisol suborders varied in their susceptibility to taxonomic change (Figure 7, Figures 8 and 9). Orthels are predominantly distributed in Interior and Western Alaska and are therefore most vulnerable to taxonomic change due to NSP loss (Figure 8). Most critically, because Orthels are not widely distributed in Northern Alaska (Figure 3), their distribution is severely restricted under all emission scenarios by mid- and late century, with late century statewide losses ranging from -59% to 54% in the low emissions scenarios

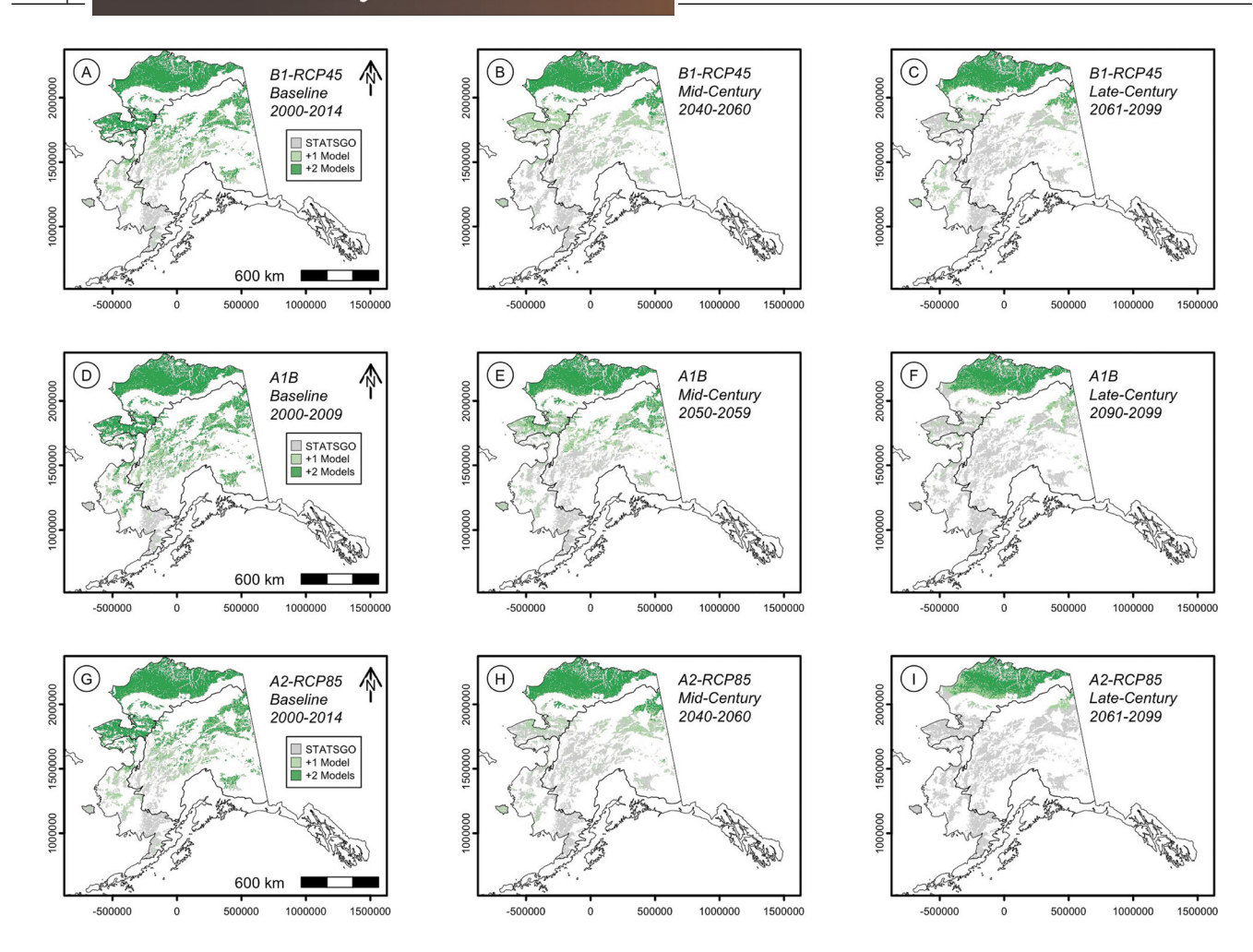


FIGURE 7 Binary representation of 1-km raster cells that contain Histels for early 21st-century baseline scenarios, and under low (Special Report on Emissions Scenario [SRES] B1, Representative Concentration Pathway [RCP] 4.5), moderate (SRES A1B), and high (SRES A2, RCP 8.5) emission scenarios. The gray areas contain Histels in the STATSGO dataset, while areas in blue have either one or two near-surface permafrost (NSP) models predicting Histel presence (regardless of prevalence). Note that there are exactly two data sources in each emissions scenario category (Section 2.1.2).

to -74 to -79% in moderate emissions scenarios and -74% to -90% in high emissions scenarios. In contrast, Turbels and Histels have a significant proportion of their aerial extent in Northern Alaska (Figures 7 and 9), and thus they experience more moderate statewide losses by late century even under the high emission scenarios (-27% to -42% for Turbels and -39% to -48% for Histels) and remain relatively widely distributed in Northern Alaska (Figures 7 and 9).

4 | DISCUSSION

4.1 | Baselines and projections of 21st-century Gelisol extent in Alaska

Based on the data from SSURGO-certified areas in Alaska, it is clear that many models have difficulty representing NSP distribution in Southern, Western, and some portions

of Interior Alaska (Figure 4). Notably, the greatest area of uncertainty among NSP model baseline Gelisol estimates is Western Alaska, where SSURGO data are lacking, yet NSP is known to be reasonably extensive (Jorgenson et al., 2008). In the baseline scenario, the GIPL and Pastick datasets outperformed other datasets with respect to SSURGO Gelisol distributions (Table S2). Other global-scale models not used in our analysis (Guo & Wang, 2016; Poggio et al., 2021) also do a poor job of reproducing the distribution of NSP and Gelisols in Western and Southern Alaska. Resolving these uncertainties is therefore critical at regional scales (i.e., Whitley et al., 2018) and will require significant field-based ground truthing and monitoring efforts in these regions, which are highly under sampled relative to soils in other parts of Alaska (Vitharana et al., 2017).

Our results indicate the potential for widespread susceptibility to taxonomic change in Alaskan Gelisols due to NSP loss in the 21st century across all emissions scenarios. On a

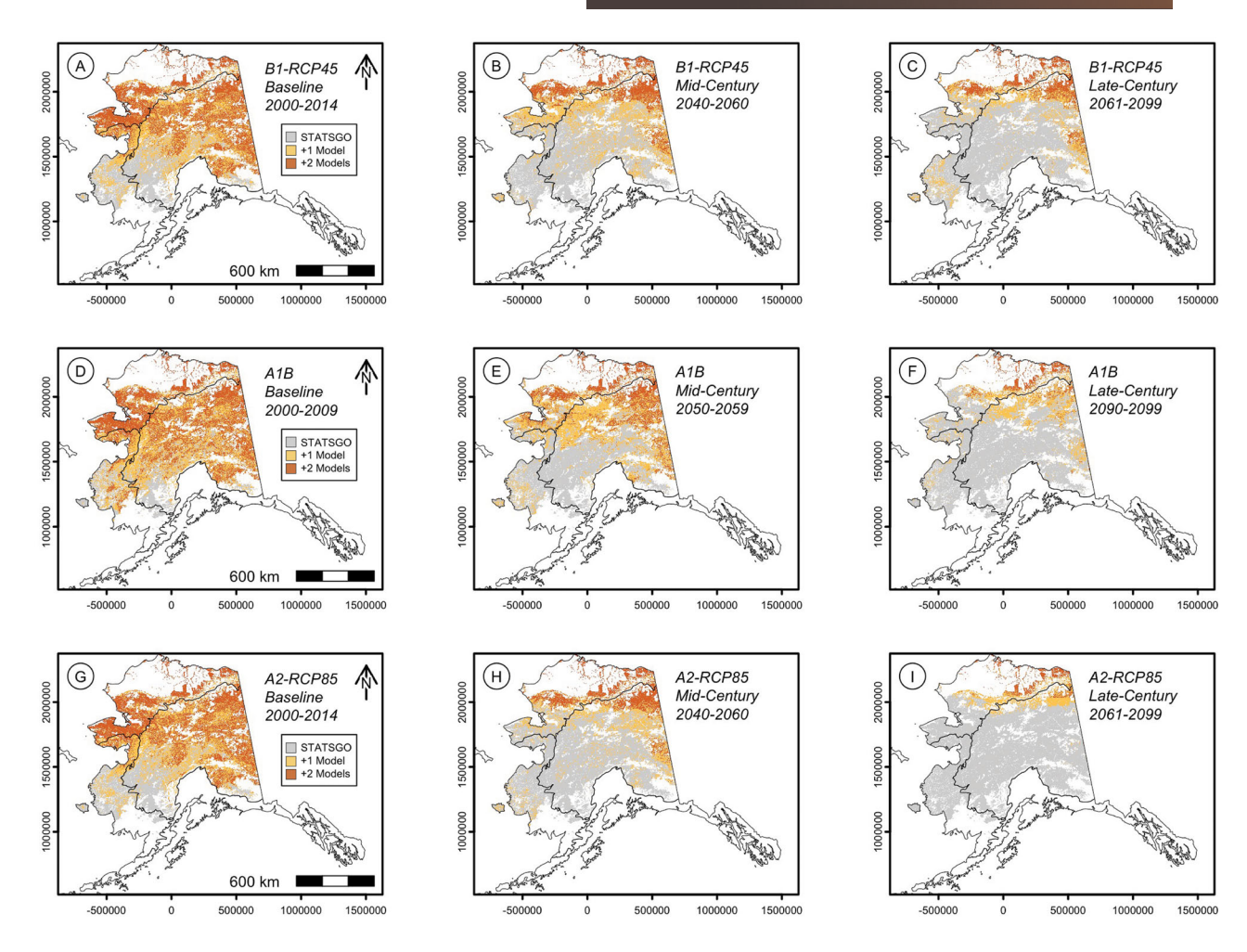


FIGURE 8 Binary representation of 1-km raster cells that contain Orthels for early 21st-century baseline scenarios, and under low (Special Report on Emissions Scenario [SRES] B1, Representative Concentration Pathway [RCP] 4.5), moderate (SRES A1B), and high (SRES A2, RCP 8.5) emission scenarios. The gray areas contain Orthels in the STATSGO dataset, while areas in blue have either one or two near-surface permafrost (NSP) models predicting Orthel presence (regardless of prevalence). Note that there are exactly two data sources in each emissions scenario category (Section 2.1.2).

statewide basis, the losses range from 41% to 69% of early 21st-century Gelisol extent across all emissions scenarios. The greatest reductions in absolute Gelisol extent by mid- and late century across all scenarios are likely to occur in Interior Alaska, while the greatest uncertainty in Gelisol taxonomic change is Western Alaska (Tables S2–S4, Figures 5 and 6). Gelisol taxonomic change in Northern Alaska is likely to be most limited in both absolute and relative extent (Figure 6). Northern Alaskan Gelisols will likely be less sensitive to taxonomic change in the 21st century because they lie predominantly in the zone of climate-driven permafrost and the NSP is more stable (Jorgenson et al., 2010). This does not mean, however, that Gelisols in Northern Alaska will not experience significant active layer deepening or the formation of taliks (unfrozen zones between the seasonally frozen active layer and permafrost), as these changes are already being observed at a much more rapid pace than predicted in some Arctic soils (Farguharson et al., 2019). Due to the differing spatial distribution of Gelisol suborders across the state of

Alaska, the greatest uncertainty in 21st-century Gelisol suborder extent lies in the Orthels of Western and Interior Alaska, as Histels and Turbels are widely distributed in Northern Alaska, where NSP is expected to remain late into the 21st century regardless of the emission scenario (Figures 7–9).

It is important to note that not all of the emission scenarios investigated here are equally likely. It now appears that the low-to-moderate emissions scenarios (represented in our work by SRES B1 and A1B and RCP 4.5) are more likely "business as usual" outcomes than the high emissions scenarios (SRES A2 and RCP 8.5; Hausfather et al., 2022; Hausfather & Peters, 2020). Therefore, our high emission scenarios should be viewed as a conservative estimate of maximum change, while the low and moderate emission scenarios represent current most probable change over the 21st century.

There are several important limitations to the potential outcomes we report here. First, scenarios of either more aggressive (SRES A1F1) or more subdued (RCP 2.5) emissions or concentration pathways would change the results

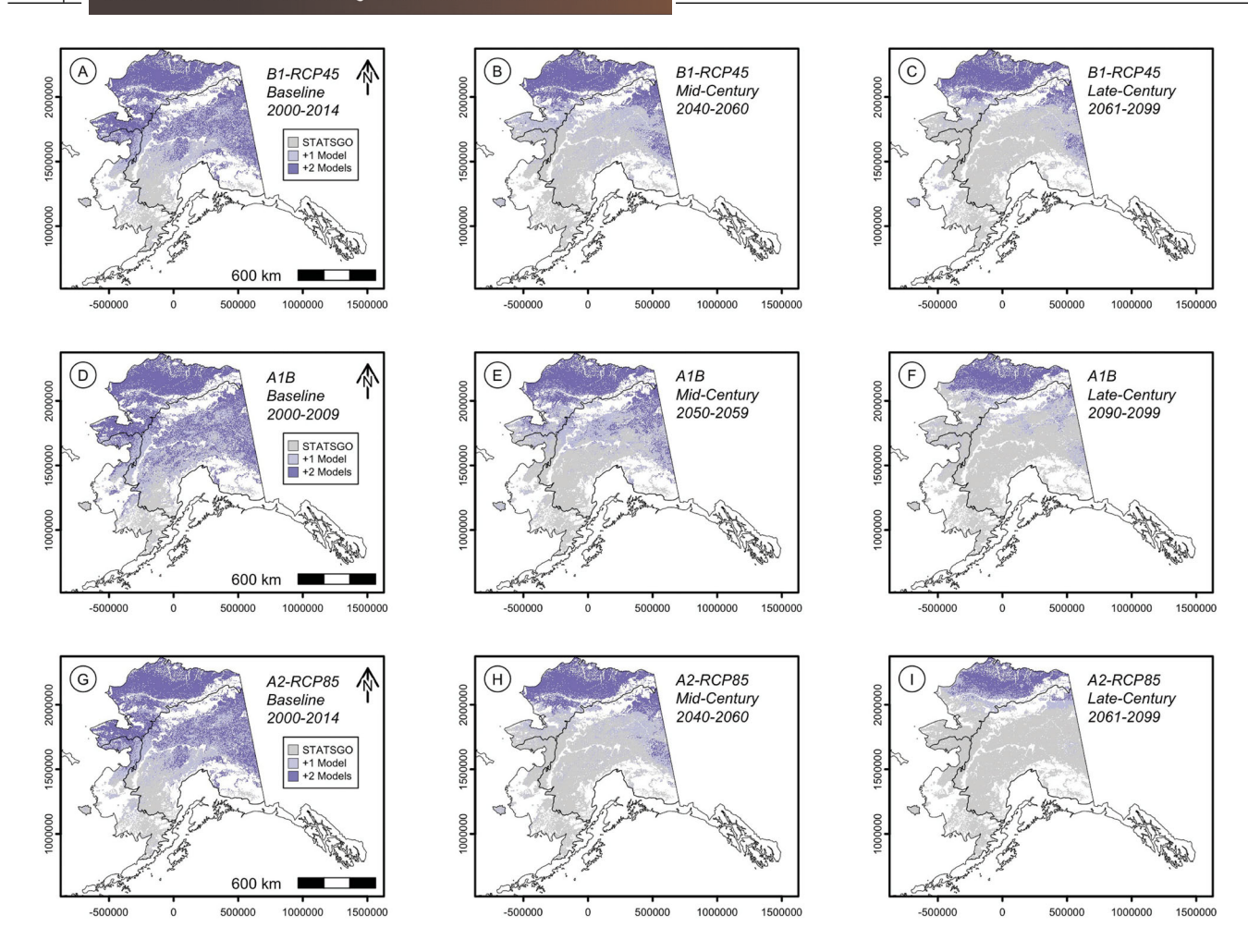


FIGURE 9 Binary representation of 1-km raster cells which contain Turbels for early 21st-century baseline scenarios, and under low (Special Report on Emissions Scenario [SRES] B1, Representative Concentration Pathway [RCP] 4.5), moderate (SRES A1B), and high (SRES A2, RCP 8.5) Emission scenarios. The gray areas contain Turbels in the STATSGO dataset, while areas in blue have either 1 or 2 near-surface permafrost (NSP) models predicting Turbel presence (regardless of prevalence). Note that there are exactly two data sources in each emissions scenario category (Section 2.1.2).

of the analysis conducted here. Nevertheless, the scenarios in our analysis span the most likely 21st-century outcomes (Hausfather & Peters et al., 2020). Additionally, the methods utilized to generate predictions of mid- and late 21st-century NSP loss in our input datasets (Pastick, GIPL, and Aalto) are driven by climate forcing over the 21st-century and do not include dynamic ecosystem properties or factors (such as fires, organic layer thickness, or vegetation type), which can have a major influence on soil thermal regimes (Anderson et al., 2019; Li et al., 2022). For example, the thickness of surficial organic materials exerts a primary control on the response of soil temperature and is an important factor in protecting NSP even as air temperatures increase (Koven et al., 2009; Jafarov & Schaefer et al., 2016). When unfrozen, organic materials are excellent thermal insulators relative to mineral soil materials, reducing the magnitude of downward heat transfer during the growing season, while they act as poor insulators in frozen state (Jorgenson et al., 2010). The combined effects of these thermal properties in frozen

and unfrozen states (known as "thermal offset"; Kudryavtsev et al., 1974) dramatically increase effectiveness in protecting NSP. The dynamic response of organic materials to environmental changes will thus also have an impact on Gelisol classification change. Finally, although the STATSGO dataset is currently the only available statewide dataset for Alaska that represents the spatial distribution of Gelisols, improved digital soil mapping products (such as a 30-m digital soil class probability map) for Alaska would enable this analysis to be further resolved spatially.

4.2 | NSP loss and permafrost-affected soil taxonomic change trends in other regions

Due to the direct linkage between NSP and permafrostaffected soil classes across soil taxonomic systems, 21stcentury NSP loss will also lead to widespread soil taxonomic change on a global scale. Therefore, although our study is restricted to Alaska in the context of US Soil Taxonomy, we can assess and compare our results to that of potential Cryosol (WRB, Canadian) taxonomic change due to NSP loss in other regions.

In early work from Canada, Tarnocai (1999) estimated changes in Cryosol area based on NSP loss over the 21st century in Canada under a 2xCO2 scenario (approximately corresponding to the current moderate-to-high emission SRES/RCP scenarios (A1B, A2, and RCP 8.5). Under these assumptions, the authors estimated that $\sim 51\%$ of the Cryosols in Canada would be susceptible to taxonomic change based on NSP loss projections. Our estimates of proportion change in Gelisols from Alaska for the moderate-to-high emission scenarios are similar but suggest slightly more extensive taxonomic change, in excess of 60% of earlycentury Gelisols under moderate-to-high emission scenarios. Tarnocai (1999) predicted this change would affect organic Cryosols (analogous to Histels in Soil Taxonomy) in Canada most significantly—due to their geographic distribution in Canada and strong association with the Hudson Bay Lowlands (Tarnocai & Bockheim, 2011). In Alaska, however, we found Orthels to be the Gelisol suborder most susceptible to taxonomic change due to their widespread distribution in Western and Interior Alaska (Figure 3).

Estimates of NSP loss across the entire northern circumpolar region have suggested changes of similar magnitude, but with important regional variability. Guo and Wang (2016), from an ensemble prediction of CMIP models, predicted an average loss of 48%–73% of early-century NSP across the northern circumpolar region as a whole in moderate-to-high emissions scenarios (RCP 4.5–RCP 8.5), with significant reductions in NSP area by 2080–2099. These predictions varied regionally for Russia (49%–76% loss in RCP 4.5–RCP 8.5), Canada (45%–68% loss in RCP 4.5–RCP 8.5), and the United States (72%–92% loss in RCP 4.5–RCP 8.5). Notably, the US-based estimates in this global scale work greatly exceed our estimates for Alaska across all scenarios, perhaps due to the significantly coarser spatial resolution than the datasets used in our analysis.

Permafrost-affected soil classes are widely distributed across the Chinese Qinghai-Tibet Plateau (QTP) or the "third pole," in conjunction with ~1 million km² of permafrost (Fang et al., 2015; Zou et al., 2017). In recent work using CMIP6 projections, Zhang et al. (2022) utilized a set of Shared Socioeconomic Pathways (SSP) scenarios (SSP 1–2.6, SSP 2–4.5, and SSP 3–7.0, and SSP 5–8.5, which broadly correspond to RCP scenarios: RCP 2.6, RCP 4.5, and RCP 8.5; Hausfather & Peters, 2020) and found the potential for NSP losses of 44% in the moderate emissions scenario (SSP 2–4.5), and 59%–71% in high emissions scenarios (SSP 3–7.0, SSP 5–8.5). Thus, NSP and permafrost-affected soil taxa are likely to become severely restricted across the QTP by the late 21st century (Zhang et al., 2022).

4.3 | Gelisols as threatened soils

The magnitude and extent of late century taxonomic changes that we have estimated here in the most probable low (136,881 to 213,853 km²) and moderate (195,623–277,691 km²) emissions scenarios is extensive by late century (Tables S2 and S3, Figures 5 and 6). There are few precedents for taxonomic change on this scale with the exception of eroded agricultural soils in the conterminous United States (estimated at greater than 460,000 km²; Fenton, 2012; Veenstra & Burras, 2012; Jelinski & Yoo, 2016). In their analysis, Amundson et al. (2003) concluded that only four soil orders in the United States have had their total undisturbed area reduced by more than 20%: Mollisols (28), Histosols (24), Vertisols (24), and Alfisols (22). Our estimates of late century taxonomic change for Gelisols result in greater proportional losses than these other soil orders by a factor of approximately 2.

Despite these large changes, by the definitions of Amundson et al. (2003), Gelisols as an order would not be considered rare (less than 10 km² total area) or endangered (less than 10 km² and loss of greater than 50% of their land area) in Alaska by 2100 due to the large extent of NSP and Gelisols that may remain in Northern Alaska by late century (Figure 6) under all emissions scenarios. However, the Gelisol order could meet the non-quantitative definition of threatened soils proposed by Drohan and Farnham (2006), given that they are undergoing significant proportional losses, as well as transformations that alter their character and function, provide significant ecosystem services and are extremely scientifically important. Additionally, although Gelisols are not currently endemic to Alaska in the United States (Bockheim, 2015), climate change is likely to result in the major loss of NSP sensitive highaltitude soils and thus leave Gelisols only endemic to Northern Alaska by the late 21st century (Knight, 2022).

Due to the sporadic and minimal coverage of SSURGO across Alaska, we cannot assess the aerial coverage of individual soil series as was done in Amundson et al. (2003), and no Gelisol orders or suborders rise to the quantitative endangered criteria of Amundson et al. (2003) at the state level. However, some Gelisol taxa may be threatened within individual LRRs. For example, Western Alaska Gelisol suborders could qualify as rare and endangered by 2100 in the high emission scenarios, with nearly complete projected losses of NSP (Table S4). Additionally, the 111 Gelisol soil series currently set up in Alaska are predominantly distributed in Southern and Interior Alaska and may become rare or extinct with NSP loss projected to be most severe in those LRRs.

Although previous efforts to identify and conserve rare and threatened soils have focused on taxa that have been altered largely due to direct human land use (Amundson et al., 2003; Drohan & Farnham, 2006), the impacts of 21st-century climate change on NSP loss and Gelisol taxonomic change have the potential to be just as widespread and more uncertain.

Additionally, although other rare or threatened soil taxa may be conserved by direct land management action, we have limited tools to stop NSP loss directly in a warming climate at large scales, despite emerging land management techniques that may slow the process (Beer et al., 2020) and systematic efforts to document rare and endemic soils (Shangguan et al., 2014).

4.4 Whence (taxonomically) go Gelisols following NSP loss?

The taxonomic disposition of Gelisols following NSP loss may depend on NSP degradation pathway—under conditions of gradual NSP loss in situ—without major land surface disturbance—Gelisols may be distributed into several other soil orders depending on their properties (Tarnocai, 1999). Conversely, conditions of severe thermokarsting or fluival and maritime degradation may lead to severe erosion and result in newly exposed fresh sediments (Rudy et al., 2017) that would classify as Entisols.

Determining a comprehensive taxonomic classification of Gelisols under conditions of in situ NSP degradation at levels below the suborder is beyond the scope of this study. However, a few broad examples at the level of suborder can be explored. With the exception of NSP presence, Histel criteria are analogous to Histosol criteria, so in the absence of NSP, Histels would become Histosols (Fibrists, Hemists, or Saprists). Mineral, permafrost-affected soils (Turbels and Orthels) present additional challenges. Prior to the addition of Gelisols to US Soil Taxonomy (Ahrens et al., 2004), 65% of the permafrost-affected soils in Alaska were classified into only two subgroups of Inceptisols: the Pergelic Cryaquepts and Ruptic-Histic Pergelic Cryaquepts (Moore & Ping, 1989). Since that time, numerous changes to non-Gelisol suborder criteria have been made in US Soil Taxonomy so that there are currently 30 great groups in five soil orders that have gelic or cryic soil temperature regimes in their criteria (Soil Survey Staff, 2022a). Nevertheless, because permafrost restricts soil drainage and many permafrost and non-permafrost soils in Alaska have features indicative of saturation and iron reduction near to the surface, it is likely that most mineral soils with aquic conditions near the surface but no longer qualifying as Gelisols would move to the Cryic or Gelic great groups of Aquic suborders of Inceptisols or Entisols. Better drained Gelisols and those that lack morphological indicators of aquic conditions near the surface after following NSP recession may move to the Cryic and Gelic suborders of Andisols, Spodosols, Mollisols, and Inceptisols, or great groups of Entisols (Gelaquents, Gelifluvents, and Gelorthents; Soil Survey Staff, 2022a).

The addition of "Cyclic" subgroups to the Gelisol suborders, which would include soils in Subgelic soil temperature

regimes that periodically have the properties of Gelisols and non-Gelisols due to NSP fluctuation, would have the advantages of providing a consistent taxonomic entity more reflective of the ecological realities of soils in the zone of discontinuous permafrost in Interior and Western Alaska. In these areas, NSP may fluctuate below requisite depths even in the absence of climatic change due to dynamic environmental factors such as fire and vegetation succession (Ping, 2013a, 2013b). Although this approach has the disadvantage of separating field morphology and classification from map unit concepts, it has been used extensively in the mapping of eroded phases of Mollisols in the central United States, which was done in order to maintain the genetic thread for users of the soil survey (Fenton, 2012).

A final taxonomic issue that may affect the reclassification of these soils following NSP loss is whether or not cryogenic structures produced when a soil had NSP were subsequently regarded as pedogenic structure for the purposes of identifying a cambic horizon (Bockheim et al., 2006). Some Gelisols undergoing NSP loss would likely fall into one of the Turbic subgroups currently set up within Cryaquepts and Gelaquepts, but it is unclear what would happen in the case that a soil did not qualify for cambic criteria (such as in a sandy soil). In that case, such a soil could become an Entisol, but there are no analogous Turbic subgroups set up in the five Gelic and Cryic great groups of Entisols (Gelaquents, Cryaquents, Gelifluvents, Cryofluvents, and Gelorthents; Soil Survey Staff, 2022a).

4.5 | Implications for mapping and soil survey in Alaska

Our analysis has important implications for initial soil mapping and re-mapping strategies in Alaska. The uneven distribution of Gelisol taxonomic change across the state of Alaska suggests that any 21st-century remapping efforts should be focused largely on Southern, Western, and Interior Alaskait is likely that soil classes will remain stable in Northern Alaska regardless of emission scenarios. In a recent study, Peng et al. (2023) suggested that most permafrost will persist in deep soils and sediments (greater than 3-m depth) across the northern circumpolar region by late century even under high emission scenarios. Given that most permafrost in Alaska is tens to hundreds of meters deep (Jorgenson et al., 2008), even under conditions of NSP loss and Gelisol classification change, it is highly likely that permafrost will persist at some depth under the landscape. Although this deep permafrost is beyond the purview of soil survey activities, depending on ground ice volume, permafrost thaw as deep as 15 m may threaten infrastructure and other land use and land management strategies (Hjort et al., 2018), and thus it may be imperative for soil scientists completing initial mapping or re-mapping of permafrost landscapes to construct "deep permafrost" phases of non-permafrost soil taxa. These concepts could be analogous to "drained" or "eroded" phases commonly set up in some soil survey areas (Soil Survey Staff, 2017).

5 | CONCLUSIONS

The results of our analysis suggest that a significant proportion of Alaskan Gelisols (15%–53% by 2040–2060, 41%–69% by 2061–2099) is susceptible to classification change in the 21st century. The drivers of much of this taxonomic change will come from Gelisols in Interior and Western Alaska, with Gelisols in Northern Alaska likely retaining permafrost within the requisite depth to avoid classification change by late century. Gelisols in Southern Alaska and Orthels throughout the state are likely to undergo nearly complete taxonomic change. Our results have important implications for the completion of soil survey in permafrost-affected landscapes, particularly for projects taking place in those landscapes experiencing rapid change. Mapping units should include both permafrost and non-permafrost or deep permafrost phases to extend the lifetime and usefulness of soil surveys into the end of the century. Although our analysis is restricted to Alaska, the results are relevant across the circumpolar region as continued climatic and environmental change is likely to affect large changes in the classification of permafrost-affected soils regardless of the taxonomic system utilized.

AUTHOR CONTRIBUTIONS

Nicolas Jelinski: Conceptualization; data curation; formal analysis; methodology; software; visualization; writing—original draft; writing—review and editing. Alexander Kholodov: Resources; writing—original draft. Neal Pastick: Conceptualization; data curation; methodology; resources; writing—original draft; writing—review and editing. Michael Sousa: Formal analysis; methodology; writing—review and editing. John Galbraith: Conceptualization; writing—review and editing.

ACKNOWLEDGMENTS

The authors wish to thank three anonymous reviewers and Associate Editor Dr. D. Beaudette for their detailed and constructive comments on the original version of the manuscript. These comments lead to significant improvements in the manuscript, and their time, effort, and care are much appreciated. Additionally, the authors would like to thank (in no particular order) Mark Clark, Dr. Chien-Lu Ping, Nathan Parry, Dennis Mulligan, Cory Cole, Denise Miller, Stephanie Schmit, Jessica Lené-Ashley, and Tim Riebe for many interesting and challenging conversations. Any use of trade, firm,

or product names is for descriptive purposes only and does not imply endorsement by the US government.

CONFLICT OF INTEREST STATEMENT

The authors declare no conflicts of interest.

DATA AVAILABILITY STATEMENT

Files containing R scripts and processed data which implement the operations described in the manuscript, as well as generation of figures and tables can be found at the GitHub repository for this project: https://github.com/jelinskilab-pedology/M007-jelinski-gelisol-change-ak.10.1002-saj2.20729 or the Zenodo archive at: https://zenodo.org/doi/10.5281/zenodo.13255023. This DOI represents all release versions, and will always resolve to the latest one. Note that the Zenodo archive does not include binary files associated with the release (in this case.zip files containing processed spatial data), which must be accessed through the GitHub release.

ORCID

N. A. Jelinski https://orcid.org/0000-0003-3348-6900
N. J. Pastick https://orcid.org/0000-0002-8169-3018
A. L. Kholodov https://orcid.org/0000-0002-7878-8008
M. J. Sousa https://orcid.org/0000-0002-5796-6549
J. M. Galbraith https://orcid.org/0000-0003-4097-366X

REFERENCES

Aalto, J., Karjalainen, O., Hjort, J., & Luoto, M. (2018). Statistical forecasting of current and future circum-Arctic ground temperatures and active layer thickness. *Geophysical Research Letters*, 45(10), 4889–4898.

Aandahl, A. R. (1958). Soil survey interpretation-theory and purpose. Soil Science Society of America Journal, 22(2), 152–154. https://doi.org/10.2136/sssaj1958.03615995002200020016x

Ahrens, R. J., Bockheim, J. G., & Ping, C.-L. (2004). The Gelisol order in soil taxonomy. In J. M. Kimble (Ed.), *Cryosols: Permafrost-affected soils* (pp. 627–635). Springer. https://doi.org/10.1007/978-3-662-06429-0_32

Amundson, R., Guo, Y., & Gong, P. (2003). Soil diversity and land use in the United States. *Ecosystems*, *6*(5), 470–482. https://doi.org/10.1007/s10021-002-0160-2

Anderson, J. E., Douglas, T. A., Barbato, R. A., Saari, S., Edwards, J. D., & Jones, R. M. (2019). Linking vegetation cover and seasonal thaw depths in Interior Alaska permafrost terrains using remote sensing. *Remote Sensing of Environment*, 233(November), 111363. https://doi.org/10.1016/j.rse.2019.111363

Beer, C., Zimov, N., Olofsson, J., Porada, P., & Zimov, S. (2020). Protection of permafrost soils from thawing by increasing herbivore density. *Scientific Reports*, 10(1), 4170. https://doi.org/10.1038/s41598-020-60938-y

Bockheim, J. G. (2015). Global distribution of cryosols with mountain permafrost: An overview. *Permafrost and Periglacial Processes*, 26(1), 1–12. https://doi.org/10.1002/ppp.1830

- Bockheim, J. G., Mazhitova, G., Kimble, J. M., & Tarnocai, C. (2006). Controversies on the genesis and classification of permafrost-affected soils. *Geoderma*, 137(1), 33–39. https://doi.org/10.1016/j.geoderma. 2006 08 019
- Bockheim, J. G., & Tarnocai, C. (1998). Recognition of cryoturbation for classifying permafrost-affected soils. *Geoderma*, 81(3), 281–293. https://doi.org/10.1016/S0016-7061(97)00115-8
- Clark, M. H. (2012). Description of Alaska STATSGO metadata. USDA-NRCS.
- Drohan, P. J., & Farnham, T. J. (2006). Protecting life's foundation: A proposal for recognizing rare and threatened soils. Soil Science Society of America Journal, 70(6), 2086–2096. https://doi.org/10.2136/sssaj2005.0274
- Fang, H.-B., Zhao, L., Wu, X.-D., Zhao, Y.-G., Zhao, Y.-H., & Hu, G.-J. (2015). Soil taxonomy and distribution characteristics of the permafrost region in the Qinghai-Tibet Plateau, China. *Journal of Mountain Science*, 12(6), 1448–1459. https://doi.org/10.1007/s11629-014-3133-y
- Farquharson, L. M., Romanovsky, V. E., Cable, W. L., Walker, D. A., Kokelj, S. V., & Nicolsky, D. (2019). Climate change drives widespread and rapid thermokarst development in very cold permafrost in the Canadian High Arctic. *Geophysical Research Letters*, 46(12), 6681–6689.
- Fenton, T. E. (2012). The impact of erosion on the classification of mollisols in Iowa. *Canadian Journal of Soil Science*, 92(3), 413–418. https://doi.org/10.4141/cjss2010-042
- French, H., & Shur, Y. (2010). The principles of cryostratigraphy. Earth-Science Reviews, 101(3-4), 190-206. https://doi.org/10.1016/ i.earscirev.2010.04.002
- Genet, H., He, Y., David McGuire, A., Zhuang, Q., Zhang, Y., Biles, F. E., D'Amore, D. V., Zhou, X., & Johnson, K. D. (2016). Terrestrial carbon modeling: Baseline and projections in upland ecosystems. In *Baseline and projected future carbon storage and greenhousegas fluxes in ecosystems of Alaska* (pp. 105–132). United States Geological Survey. https://pubs.usgs.gov/pp/1826/pp1826_chapter6.pdf
- Grosse, G., Goetz, S., McGuire, A. D., Romanovsky, V. E., & Schuur, E. A. G. (2016). Changing permafrost in a warming world and feedbacks to the Earth system. *Environmental Research Letters*, 11(4), 040201. https://doi.org/10.1088/1748-9326/11/4/040201
- Canadian Soil Classification Working Group. (1998). The Canadian system of soil classification (3rd ed.). Agriculture and Agri-Food Canada.
- Guo, D., & Wang, H. (2016). Cmip5 permafrost degradation projection: A comparison among different regions. *Journal of Geophysical Research: Atmospheres*, 121(9), 4499–4517. https://doi.org/10.1002/2015JD024108
- Harris, S. A., Brouchkov, A., & Guodong, C. (2018). Geocryology: Characteristics and use of frozen ground and permafrost landforms. CRC Press.
- Hausfather, Z., Marvel, K., Schmidt, G. A., Nielsen-Gammon, J. W., & Zelinka, M. (2022). Climate simulations: Recognize the 'hot model' problem. *Nature*, 605(7908), 26–29. https://doi.org/10.1038/d41586-022-01192-2
- Hausfather, Z., & Peters, G. P. (2020). Emissions—The 'business as usual' story is misleading. *Nature*, 577(7792), 618–620. https://doi. org/10.1038/d41586-020-00177-3
- Hengl, T., de Jesus, J. M., MacMillan, R. A., Batjes, N. H., Heuvelink, G. B. M., Ribeiro, E., Samuel-Rosa, A., Kempen, B., Leenaars, J. G.,

- Walsh, M. G., & Gonzalez, M. R. (2014). SoilGrids1km—Global soil information based on automated mapping. *PLoS ONE*, *9*(8), e105992. https://doi.org/10.1371/journal.pone.0105992
- Hijmans, R. J., Bivand, R., Pebesma, E., & Sumner, M. D. (2023). Terra: Spatial data analysis. https://cran.r-project.org/web/packages/terra/ index.html
- Hijmans, R. J., Cameron, S. E., Parra, J. L., Jones, P. G., & Jarvis, A. (2005). Very high resolution interpolated climate surfaces for global land areas. *International Journal of Climatology*, 25(15), 1965–1978. https://doi.org/10.1002/joc.1276
- Hjort, J., Karjalainen, O., Aalto, J., Westermann, S., Romanovsky, V. E., Nelson, F. E., Etzelmüller, B., & Luoto, M. (2018). Degrading permafrost puts arctic infrastructure at risk by mid-century. *Nature Communications*, 9(1), 5147. https://doi.org/10.1038/s41467-018-07557-4
- Hjort, J., Streletskiy, D., Doré, G., Wu, Q., Bjella, K., & Luoto, M. (2022). Impacts of permafrost degradation on infrastructure. *Nature Reviews Earth & Environment*, 3, 24–38. https://doi.org/10.1038/s43017-021-00247-8
- Hugelius, G., Strauss, J., Zubrzycki, S., Harden, J. W., Schuur, E. A. G., Ping, C.-L., Schirrmeister, L., Grosse, G., Michaelson, G. J., Koven, C. D., O'Donnell, J. A., Elberling, B., Mishra, U., Camill, P., Yu, Z., Palmtag, J., & Kuhry, P. (2014). Estimated stocks of circumpolar permafrost carbon with quantified uncertainty ranges and identified data gaps. *Biogeosciences*, 11(23), 6573–6593. https://doi.org/10.5194/bg-11-6573-2014
- Hugelius, G., Tarnocai, C., Broll, G., Canadell, J. G., Kuhry, P., & Swanson, D. K. (2013). The Northern Circumpolar Soil Carbon database: Spatially distributed datasets of soil coverage and soil carbon storage in the northern permafrost regions. *Earth System Science Data*, 5(1), 3–13. https://doi.org/10.5194/essd-5-3-2013
- Jafarov, E. E., Marchenko, S. S., & Romanovsky, V. E. (2012). Numerical modeling of permafrost dynamics in Alaska using a high spatial resolution dataset. *The Cryosphere*, *6*(3), 613–624. https://doi.org/10.5194/tc-6-613-2012
- Jafarov, E. E., & Schaefer, K. (2016). The importance of a surface organic layer in simulating permafrost thermal and carbon dynamics. *The Cryosphere*, 10(1), 465–475. https://doi.org/10.5194/tc-10-465-2016
- Jelinski, N. A., & Yoo, K. (2016). The distribution and genesis of eroded phase soils in the conterminous United States. *Geoderma*, 279, 149– 164.
- Jones, A., Stolbovoy, V., Tarnocai, C., Broll, G., Spaargaren, O., & Montanarella, L. (Eds.). (2009). Soil atlas of the northern circumpolar region. European Commission, Office for Official Publications of the European Communities. https://esdac.jrc.ec.europa.eu/content/soil-atlas-northern-circumpolar-region
- Jorgenson, M. T., Romanovsky, V., Harden, J., Shur, Y., O'Donnell, J., Schuur, E. A. G., Kanevskiy, M., & Marchenko, S. (2010). Resilience and vulnerability of permafrost to climate change. *Canadian Journal* of Forest Research, 40(7), 1219–1236. https://doi.org/10.1139/X10-060
- Jorgenson, M. T., Yoshikawa, K., Kanevskiy, M. Z., Shur, Y. L., Romanovsky, V. E., Marchenko, S. S., Grosse, G., Brown, J., & Jones, B. (2008). Permafrost characteristics of Alaska. In *Proceedings of the ninth international conference on permafrost* (pp. 121–1222). University of Alaska-Fairbanks: Institute for Northern Engineering. https://catalog.northslopescience.org/dataset/54

- Knight, J. (2022). Scientists' warning of the impacts of climate change on mountains. *PeerJ*, 10(October), e14253. https://doi.org/10.7717/ peerj.14253
- Koven, C., Friedlingstein, P., Ciais, P., Khvorostyanov, D., Krinner, G., & Tarnocai, C. (2009). On the formation of high-latitude soil carbon stocks: Effects of cryoturbation and insulation by organic matter in a land surface model. *Geophysical Research Letters*, 36(21), L21501. https://doi.org/10.1029/2009GL040150
- Kudryavtsev, V. A., Garagula, L. S., Kondrat'yeva, K. A., & Melamed, V. G. (1974). Osnovy merzlotnogo prognoza. MGU.
- Li, X., Jin, H., Wang, H., Jin, X., Bense, V. F., Marchenko, S. S., He, R., Huang, Y., & Luo, D. (2022). Effects of fire history on thermal regimes of permafrost in the Northern Da Xing'anling Mountains, NE China. *Geoderma*, 410(March), 115670. https://doi.org/10.1016/j.geoderma.2021.115670
- Moore, J. P., & Ping, C. L. (1989). Classification of permafrost soils. Soil Survey Horizons, 30(4), 98–104. https://doi.org/10.2136/sh1989. 4.0098
- Moss, R. H., Edmonds, J. A., Hibbard, K. A., Manning, M. R., Rose, S. K., Van Vuuren, D. P., Carter, T. R., Emori, S., Kainuma, M., Kram, T., Meehl, G. A., Mitchell, J. F. B., Nakicenovic, N., Riahi, K., Smith, S. J., Stouffer, R. J., Thomson, A. M., Weyant, J. P., & Wilbanks, T. J. (2010). The next generation of scenarios for climate change research and assessment. *Nature*, 463(7282), 747–756. https://doi.org/10.1038/nature08823
- Osterkamp, T. E., Jorgenson, M. T., Schuur, E. A. G., Shur, Y. L., Kanevskiy, M. Z., Vogel, J. G., & Tumskoy, V. E. (2009). Physical and ecological changes associated with warming permafrost and thermokarst in Interior Alaska. *Permafrost and Periglacial Processes*, 20(3), 235–256. https://doi.org/10.1002/ppp.656
- Pastick, N. J., Jorgenson, M. T., Goetz, S. J., Jones, B. M., Wylie, B. K., Minsley, B. J., Genet, H., Knight, J. F., Swanson, D. K., & Jorgenson, J. C. (2019). Spatiotemporal remote sensing of ecosystem change and causation across Alaska. *Global Change Biology*, 25(3), 1171–1189. https://doi.org/10.1111/gcb.14279
- Pastick, N. J., Jorgenson, M. T., Wylie, B. K., Nield, S. J., Johnson, K. D., & Finley, A. O. (2015). Distribution of near-surface permafrost in Alaska: Estimates of present and future conditions. *Remote Sensing of Environment*, 168(October), 301–315. https://doi.org/10.1016/j.rse.2015.07.019
- Peng, X., Zhang, T., Frauenfeld, O. W., Mu, C., Wang, K., Wu, X., Guo, D., Luo, J., Hjort, J., Aalto, J., Karjalainen, O., & Luoto, M. (2023). Active layer thickness and permafrost area projections for the 21st century. *Earth's Future*, 11(8), e2023EF003573. https://doi.org/10.1029/2023EF003573
- Peplau, T., Schroeder, J., Gregorich, E., & Poeplau, C. (2022). Subarctic soil carbon losses after deforestation for agriculture depend on permafrost abundance. *Global Change Biology*, 28(17), 5227–5342. https://doi.org/10.1111/gcb.16307
- Ping, C. L. (2013a). Gelisols: Part I. Cryogenesis and state factors of formation. Soil Horizons, 54(3), 1–5. https://doi.org/10.2136/sh2013-54-3-gc
- Ping, C. L. (2013b). Gelisols: Part II. Classification and related issues. Soil Horizons, 54(4), 1–4. https://doi.org/10.2136/sh2013-54-4-gc
- Poggio, L., Sousa, L. M. D., Batjes, N. H., Heuvelink, G. B. M., Kempen, B., Ribeiro, E., & Rossiter, D. (2021). SoilGrids 2.0: Producing soil information for the globe with quantified spatial uncertainty. *Soilless*, 7(1), 217–240. https://doi.org/10.5194/soil-7-217-2021

- PRISM Climate Group at Oregon State University. (n.d.). https://prism. oregonstate.edu/
- Rieger, S. (1983). The genesis and classification of cold soils. Academic Press.
- Romanovsky, V. E., Smith, S. L., Isaksen, K., Shiklomanov, N. I., Kholodov, A. L., Christiansen, H. H., Drozdov, D. S., Malkova, G. V., & Marchenko, S. S. (2017). Terrestrial permafrost. In J. Richter-Menge, J. E. Overland, J. T. Mathis, & E. Osborne (Eds.), Arctic report card 2017. US National Oceanic and Atmospheric Administration. https://arctic.noaa.gov/report-card/report-card-2017/terrestrialpermafrost/
- Rudy, A. C. A., Lamoureux, S. F., Kokelj, S. V., Smith, I. R., & England, J. H. (2017). Accelerating thermokarst transforms ice-cored terrain triggering a downstream cascade to the ocean. *Geophysical Research Letters*, 44(21), 11, 080–11, 087. https://doi.org/10.1002/ 2017GL074912
- Schuur, E. A. G., & Mack, M. C. (2018). Ecological response to permafrost thaw and consequences for local and global ecosystem services. *Annual Review of Ecology, Evolution, and Systematics*, 49(1), 279–301. https://doi.org/10.1146/annurev-ecolsys-121415-032349
- Shangguan, W., Gong, P., Liang, L., Dai, Y. J., & Zhang, K. (2014). Soil diversity as affected by land use in China: Consequences for soil protection. *The Scientific World Journal*, 2014, 1–12. https://doi.org/10. 1155/2014/913852
- Snover, A. K., Mauger, G. S., Whitely Binder, L. C., Krosby, M., & Tohver, I. (2013). Making Sense of the new climate change scenarios. In *Climate change impacts and adaptation in Washington state: Technical summaries for decision makers* (State of knowledge report prepared for the Washington State Department of Ecology). University of Washington: Climate Impacts Group. http://cses.washington.edu/db/pdf/snoveretalsok816.pdf
- Staff, Soil Science Division. (2017). Soil survey manual (USDA Handbook 18). U.S. Government Printing Office.
- Staff, Soil Survey. (2022a). *Keys to soil taxonomy* (13th ed.). USDA-NRCS. https://www.nrcs.usda.gov/resources/guides-and-instructions/keys-to-soil-taxonomy
- Staff, Soil Survey. (2022b). State soil geographic database (Statsgo2) for Alaska. https://www.nrcs.usda.gov/resources/data-and-reports/description-of-statsgo2-database
- Staff, Soil Survey. (2022c). The Gridded National Soil Survey Geographic (gNATSGO) Database for Alaska. https://nrcs.app.box.com/ v/soils
- Tarnocai, C. (1999). The effect of climate warming on the carbon balance of cryosols in Canada. *Permafrost and Periglacial Processes*, 10, 251–263.
- Tarnocai, C., & Bockheim, J. (2011). Cryosolic soils of Canada: Genesis, distribution, and classification. *Canadian Journal of Soil Science*, 91(5), 749–762. https://doi.org/10.4141/cjss10020
- Tarnocai, C., Kimble, J. M., Swanson, D. K., Goryachkin, S. V., Naumov, Y. M., Stolbovoi, V., Jakobsen, B., Broll, G., Montanarella, L., Arnoldussen, A., Arnalds, O., & Yli-Halla, M. (2002). Northern circumpolar soils map, version 1 [Data Set]. University of Colorado-Boulder: National Snow and Ice Data Center. https://doi.org/10.7265/eb1s-4551
- Team, R Core. (2023). R: A language and environment for statistical computing. R Foundation for Statistical Computing. https://www.Rproject.org/

- USDA-NRCS. (2022). Major land resource area (MLRA). NRCS Soils. https://www.nrcs.usda.gov/wps/portal/nrcs/detail/soils/survey/ geo/?cid=nrcs142p2_053624
- USDA-NRCS. (2023). Soil interpretations. In National soil survey handbook. USDA-NRCS. https://www.nrcs.usda.gov/resources/ guides-and-instructions/national-soil-survey-handbook
- van Everdingen, R. O. (2005). Multi-language glossary of permafrost and related ground-ice terms (revised). International Permafrost Association.
- Veenstra, J. J., & Burras, C. L. (2012). Effects of agriculture on the classification of Black soils in the Midwestern United States. Canadian Journal of Soil Science, 92(3), 403-411.
- Vitharana, U. W. A., Mishra, U., Jastrow, J. D., Matamala, R., & Fan, Z. (2017). Observational needs for estimating Alaskan soil carbon stocks under current and future climate. Journal of Geophysical Research: Biogeosciences, 122(2), 415–429. https://doi.org/10.1002/ 2016JG003421
- Walsh, J. E., Chapman, W. L., Romanovsky, V., Christensen, J. H., & Stendel, M. (2008). Global climate model performance over Alaska and Greenland. Journal of Climate, 21(23), 6156-6174. https://doi. org/10.1175/2008JCLI2163.1
- Whitley, M., Frost, G., Jorgenson, M., Macander, M., Maio, C., & Winder, S. (2018). Assessment of LiDAR and spectral techniques for high-resolution mapping of sporadic permafrost on the Yukon-Kuskokwim Delta, Alaska. Remote Sensing, 10(2), 258. https://doi. org/10.3390/rs10020258
- WRB, IUSS Working Group. (2022). World reference base for soil resources. International soil classification system for naming soils and creating legends for soil maps (4th ed.). International Union of Soil Sciences (IUSS).
- Yi, Y., & Kimball, J. S. (2020). Arctic-Boreal Vulnerability Experiment (ABoVE): Active layer thickness from remote sensing permafrost model, Alaska, 2001-2015. ORNL DAAC. https://doi.org/10.3334/ ORNLDAAC/1760

- Yi, Y., Kimball, J. S., Chen, R. H., Moghaddam, M., Reichle, R. H., Mishra, U., Zona, D., & Oechel, W. C. (2018). Characterizing permafrost active layer dynamics and sensitivity to landscape spatial heterogeneity in Alaska. The Cryosphere, 12(1), 145-161. https://doi. org/10.5194/tc-12-145-2018
- Yi, Y., Kimball, J. S., Rawlins, M. A., Moghaddam, M., & Euskirchen, E. S. (2015). The role of snow cover affecting boreal-arctic soil freezethaw and carbon dynamics. Biogeosciences, 12(19), 5811-5829. https://doi.org/10.5194/bg-12-5811-2015
- Zhang, G., Nan, Z., Hu, N., Yin, Z., Zhao, L., Cheng, G., & Mu, C. (2022). Oinghai-Tibet Plateau permafrost at risk in the late 21st century. Earth's Future, 10(6), e2022EF002652. https://doi.org/10.1029/ 2022EF002652
- Zou, D., Zhao, L., Sheng, Y., Chen, J., Hu, G., Wu, T., Wu, J., Xie, C., Wu, X., Pang, Q., Wang, W., Du, E., Li, W., Liu, G., Li, J., Qin, Y., Qiao, Y., Wang, Z., Shi, J., & Cheng, G. (2017). A new map of permafrost distribution on the Tibetan Plateau. The Cryosphere, 11(6), 2527-2542. https://doi.org/10.5194/tc-11-2527-2017

SUPPORTING INFORMATION

Additional supporting information can be found online in the Supporting Information section at the end of this article.

How to cite this article: Jelinski, N. A., Pastick, N. J., Kholodov, A. L., Sousa, M. J., & Galbraith, J. M. (2024). Estimates of soil taxonomic change due to near-surface permafrost loss in Alaska. Soil Science Society of America Journal, 88, 1626-1646. https://doi.org/10.1002/saj2.20729